

Electronic nose (E-nose)

- Electronic noses are engineered to mimic the mammalian olfactory system
- Instrument designed to allow detection and classification of aroma mixtures
- Refers to the capability of reproducing human senses using sensor arrays and pattern recognition system



✓ cosmetic industry control



✓ environmental monitoring for air quality control



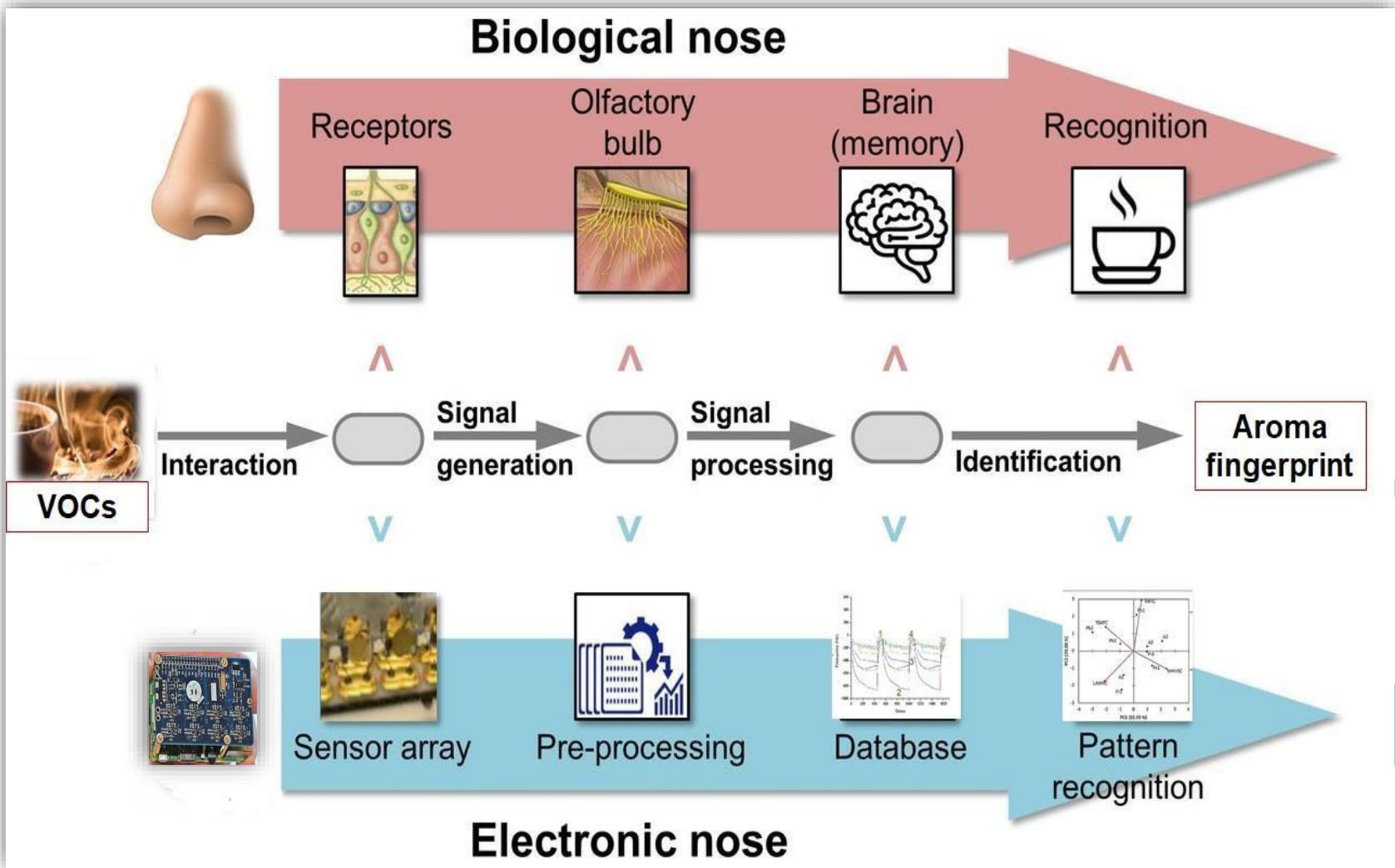
✓ food quality and safety control





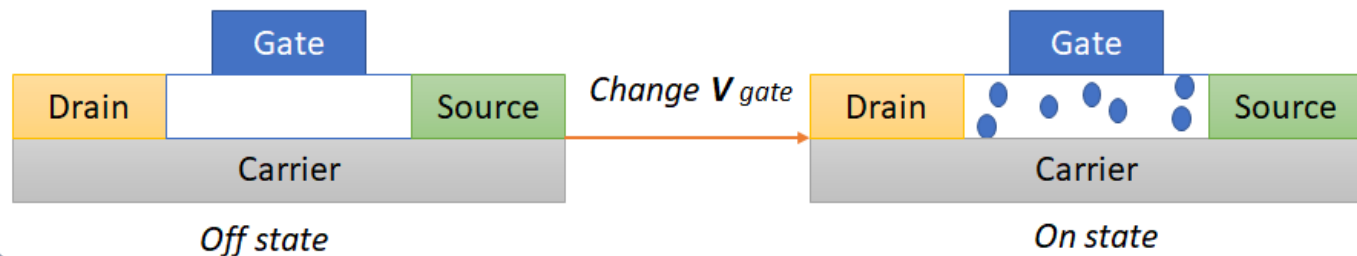
An electronic nose can now diagnose cancerous tumors. A new research have designed an electronic nose to help diagnose malignant mesothelioma early on. This nose can detect the presence of the tumor with a breath test. Malignant mesothelioma is an uncommon, usually fatal, cancerous tumour of the lining of the lung and chest cavity or lining of the abdomen (peritoneum) caused by long-term asbestos exposure. The device was designed to distinguish between benign and malignant disease and to detect the disease early. "If you catch it earlier, your chances of actually giving people the right treatment to stop it spreading are actually better," said team leader, Deborah Yates. "We tried to exclude the other asbestos diseases because it's very important from a patient's point of view that you don't pick up something that is a benign asbestos disease, so that you don't diagnose them with something that's not actually a problem," added Yates.

<https://www.thehealthsite.com/news/electronic-nose-helps-locate-deadly-tumour/>

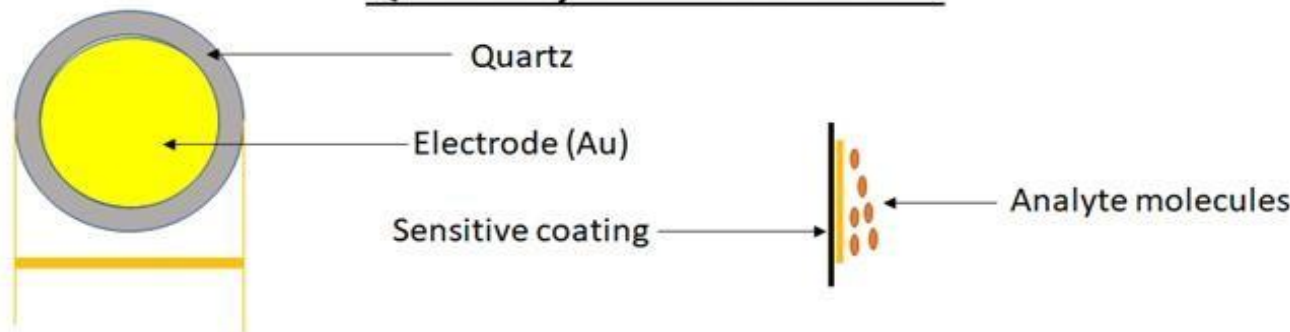


'An electronic nose is an instrument, which comprises an array of electronic chemical sensors with partial specificity and an appropriate pattern-recognition system, capable of recognizing simple or complex odors'[1]

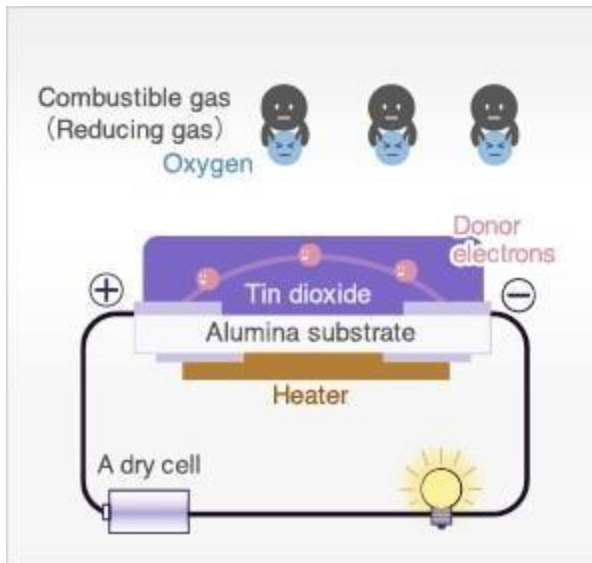
Field effect transistor



Quartz crystal microbalance

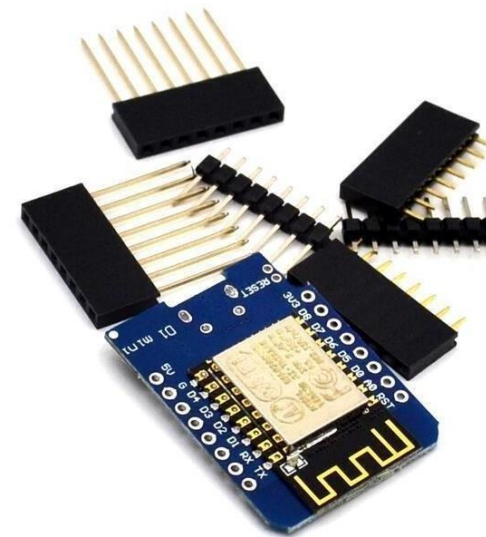


- ✓ low costs
- ✓ easy realization
- ✓ ability to work in real-time
- ✓ short analysis times



MOS SENSORS

Metal oxide semiconductors



Constituted by three main parts:

- Ceramic substrate
 - Heating wire or thermistor
 - Semiconducting metal oxides film (Zn, Co, etc.)

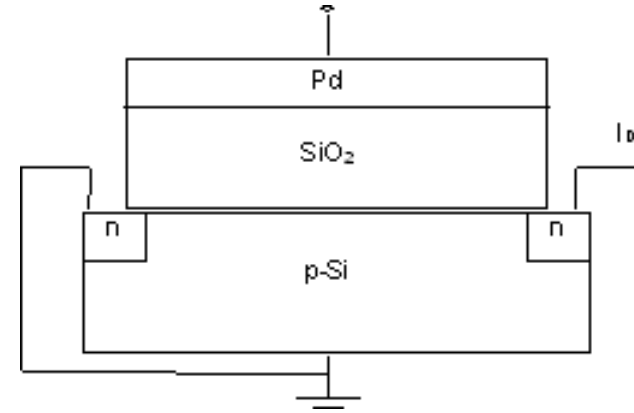
They measure conductivity changes onto the surface of the sensors induced by gases. Sensitive to combustion gases (hydrocarbons, NO, CO). Work at 300-400°C. An exchange between the gas and the oxygen on the film causes a change in resistance dependent on the adsorbed gas.

MOSFET SENSORS

Field effect metal oxides transistors

Made by 3 parts:

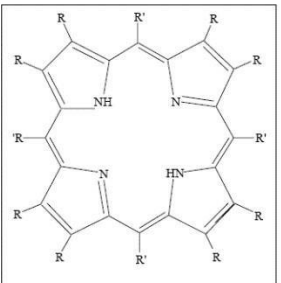
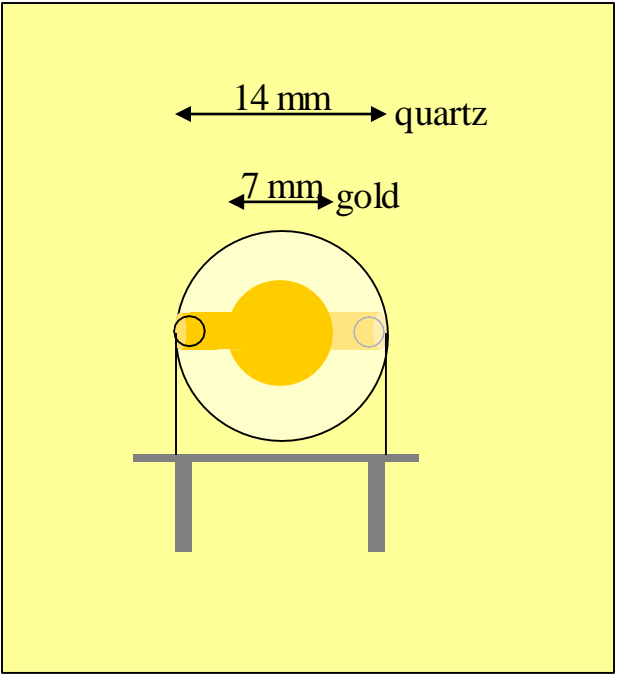
- Semiconducting Silicon
- Insulating silica layer
- Catalytic metal (Pt, Pd, etc.)



Work as a transistor at applied potential at 140-170°C. Sensitive to compounds containing hydrogen (amines, aldehydes, esters, chetons, aromatics ed alcohols). When a polar molecules interacts with the metal the electric field is modified and a change in current occurs. The device output is the voltage necessary to have the current back at the initial value.

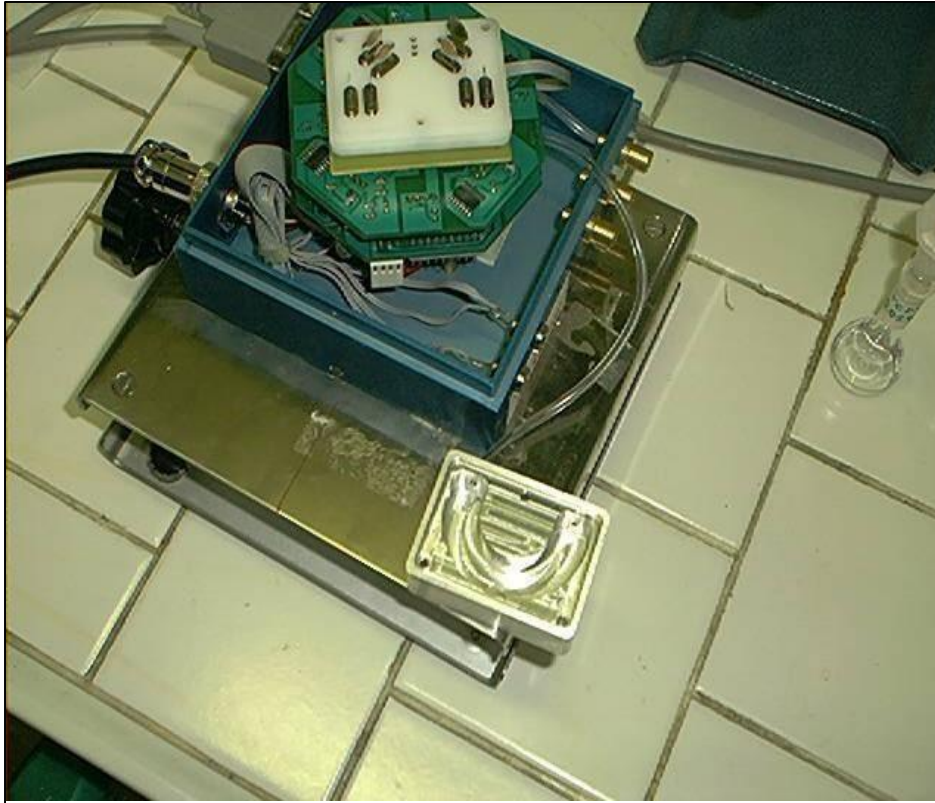
Piezoelectric System

Electronic nose

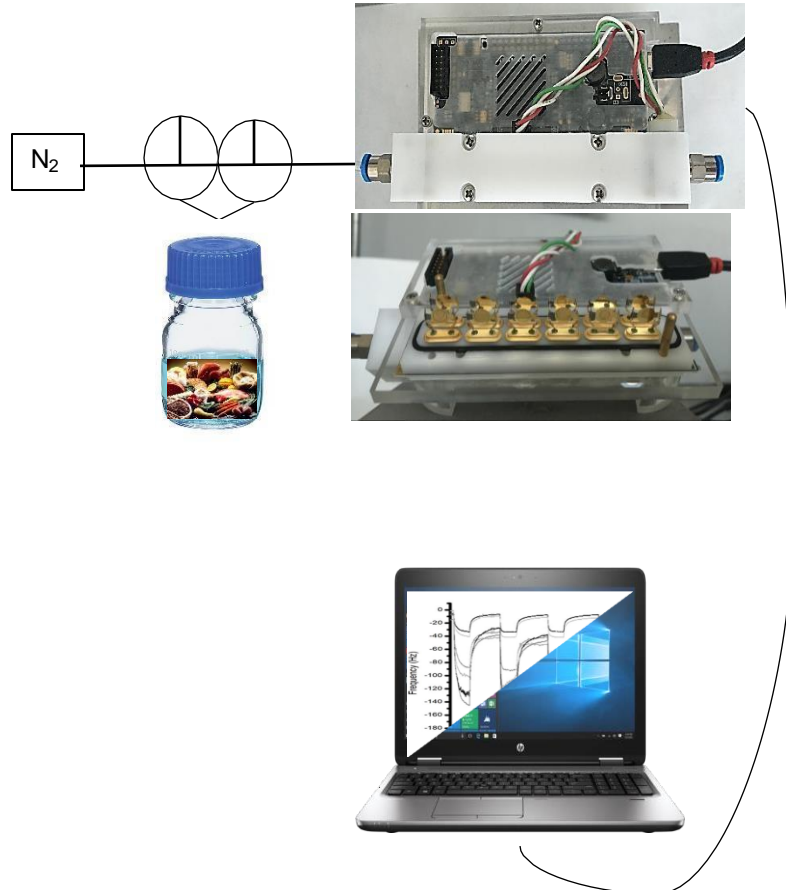


Butyloxy Tetra Phenyl Porphyrin

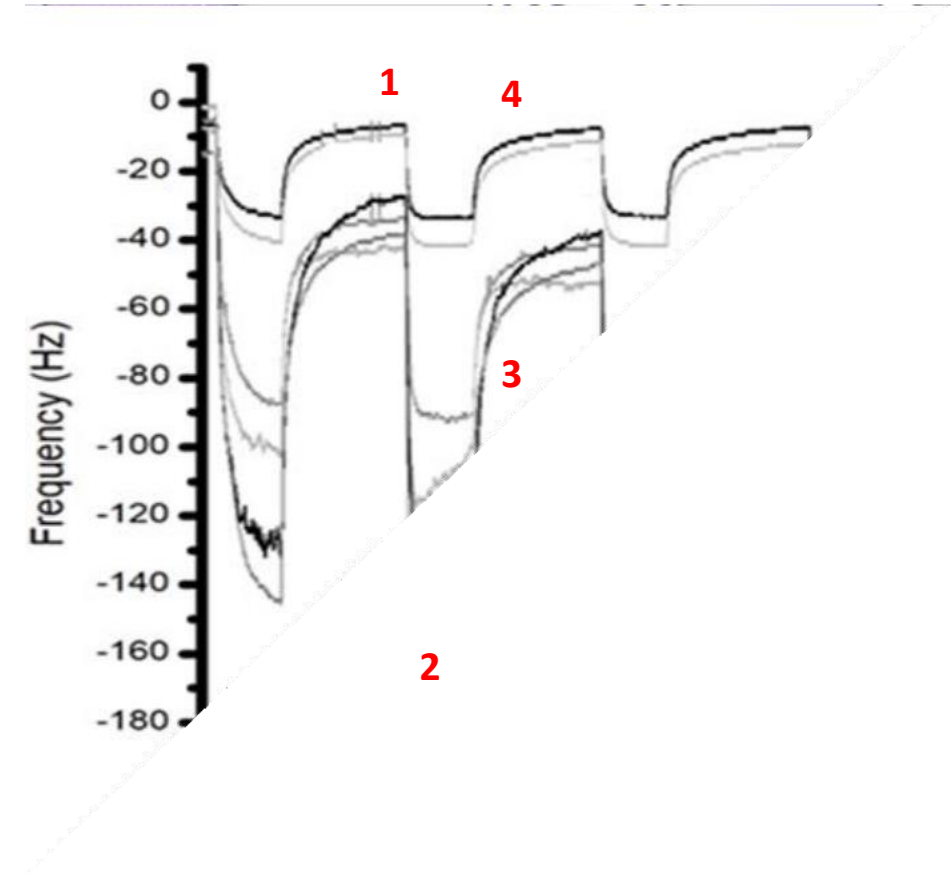
Cu
Co
Zn
Mn
Fe
Sn
Ru
Cr



Measurement system

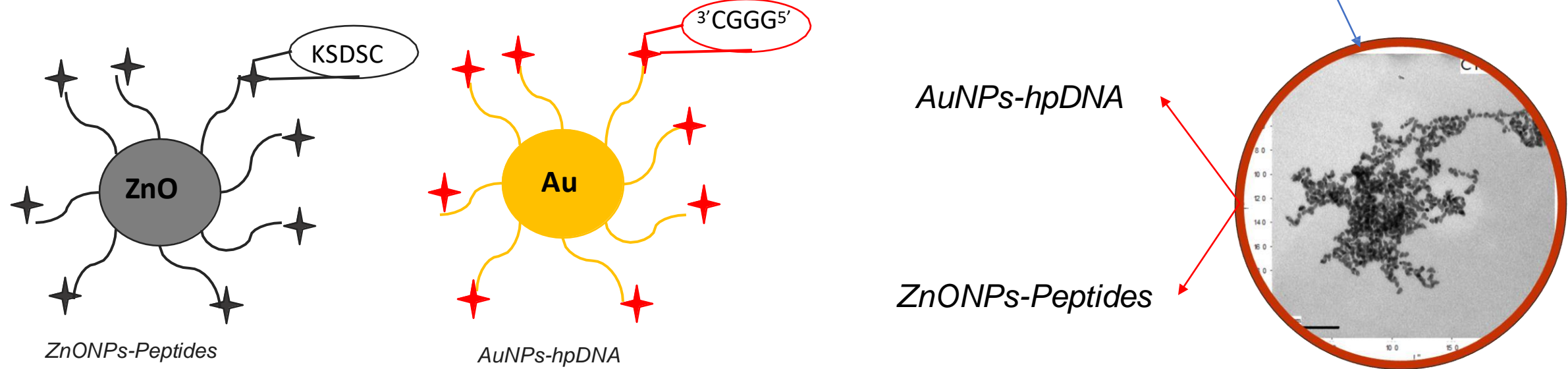
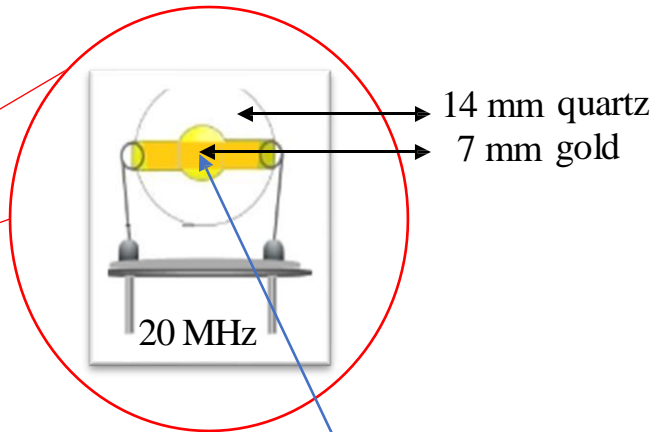
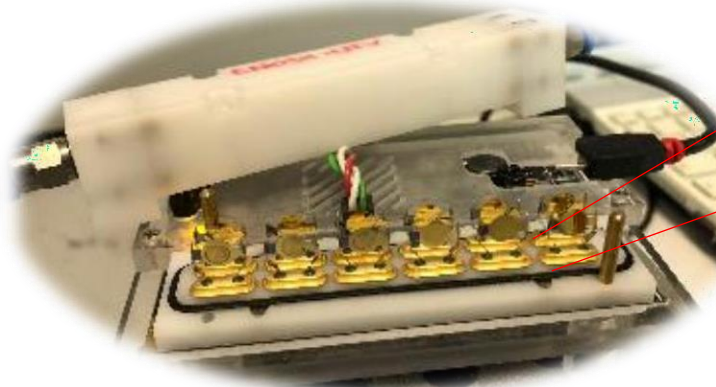
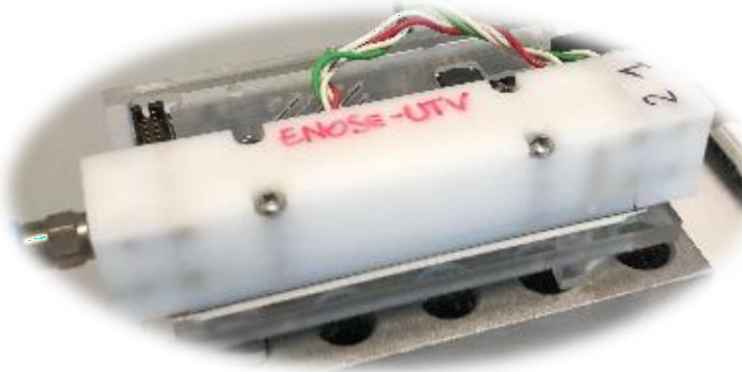


1. Start
2. Decrease
3. Equilibration
4. Baseline



Frequency signals recorded with ZnONPs-peptides testing food

Electronic nose



Electronic nose sensor arrays

GNP-Peptide based

- ✓ **AuNP-Glutathione**
- ✓ **AuNP-Cys-Gly**
- ✓ **AuNP-Cys**
- ✓ **AuNP-Thioglicolic Acid**
- ✓ **AuNP-Cys-Arg-Gln-Val-Phe**
- ✓ **AuNP-Cys-Ile-His-Asn-Pro**
- ✓ **AuNP-Cys-Ile-Gln-Pro-Val**
- ✓ **AuNP**

Porphyrin based

- ✓ **Cu-Buti-TPP**
- ✓ **Co-Buti-TPP**
- ✓ **Zn-Buti-TPP**
- ✓ **Mn-Buti-TPP**
- ✓ **Fe-Buti-TPP**
- ✓ **Sn-Buti-TPP**
- ✓ **H₂-Buti-TPP**
- ✓ **Mg-Buti-TPP**

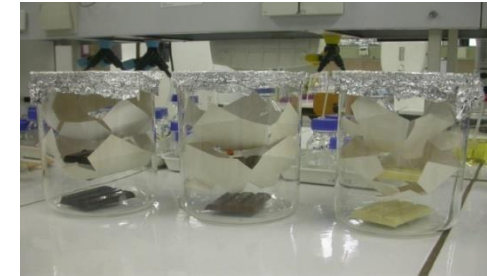


- Ⓐ **Temperature: 40°C**
- Ⓐ **Equilibration time: 10 min**
- Ⓐ **15g in 100 mL lab bottle grated and melted**
- Ⓐ **N₂ = 4 L/h**

Standard Samples
VS
Off-flavoured samples

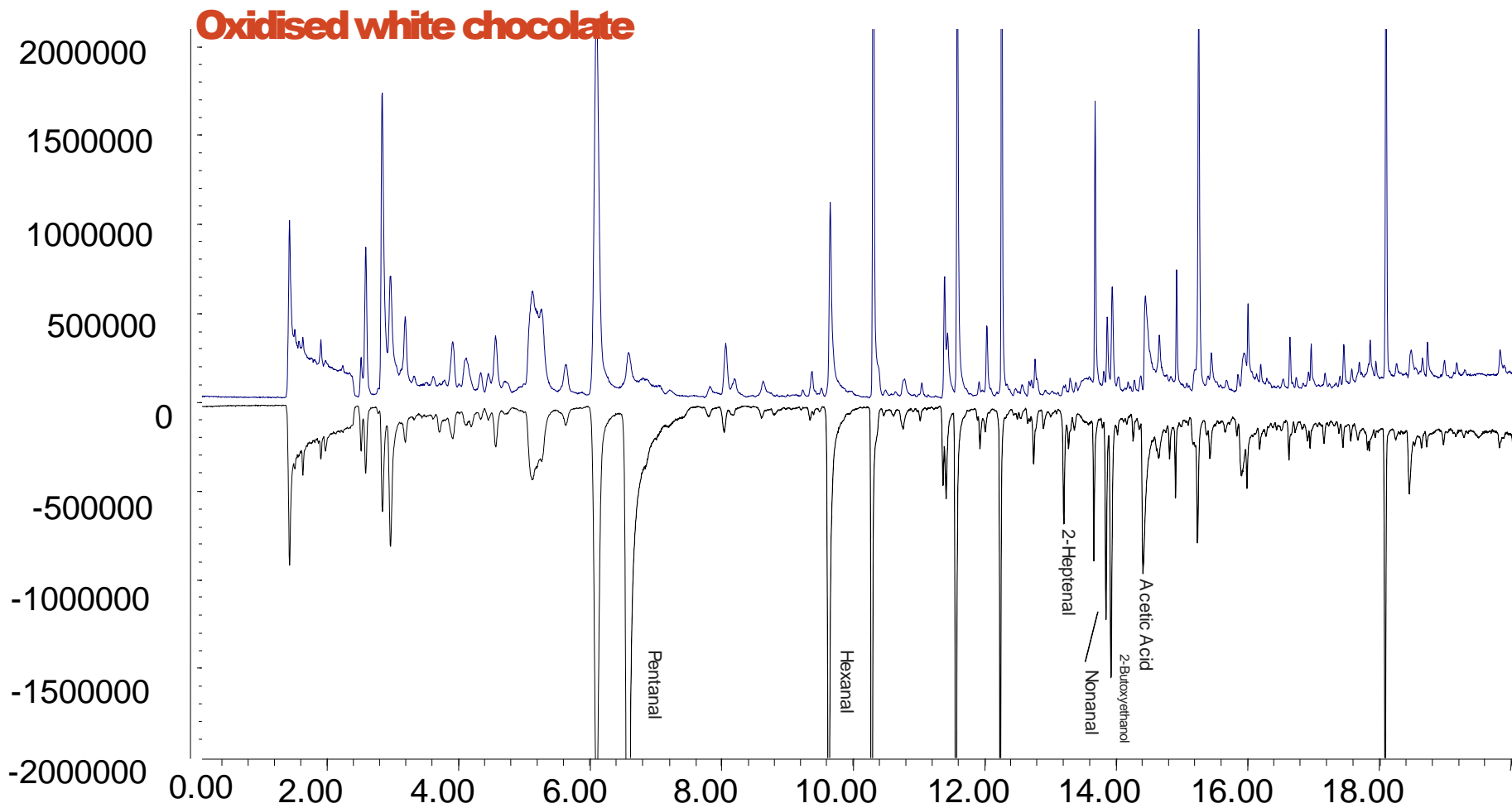
PLS-DA analysis

Off-Flavour	Process
3-methylbutanal	Fermentation volatiles
Phenylacetaldehyde	
Acetic Acid	Conching process
Tetramethylpyrazine	
2-acetylpyrrole	Roasting Process
2-nonenal	
2,4-decadienal (t,t)	Fat related (oxidation)

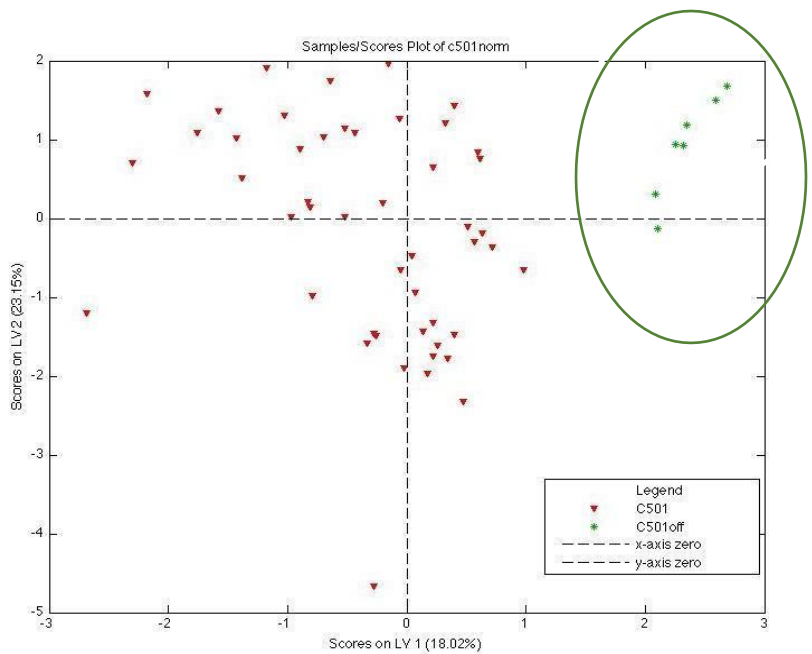


Off-flavours were preliminarily added in the cocoa butter to achieve the concentration of 125 ppm. One tea spoon of contaminated cocoa butter was then added to 400 g of chocolate to obtain an estimated final concentration in the sample of ~ 6ppm.

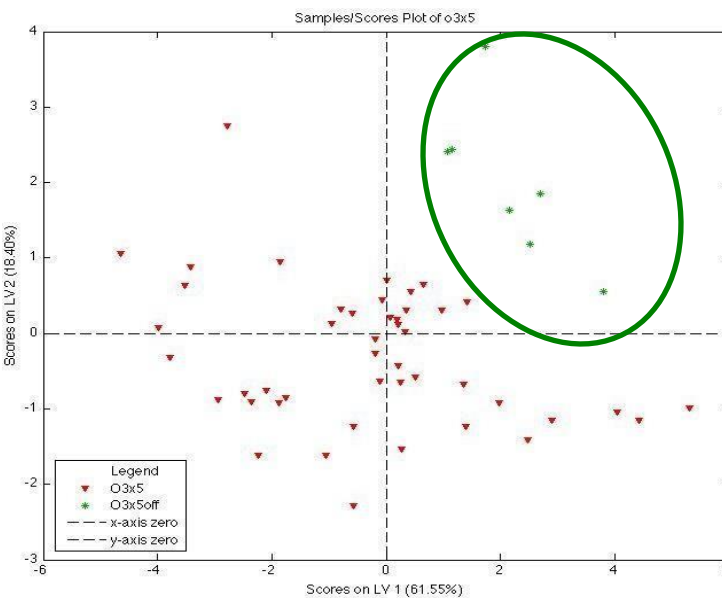
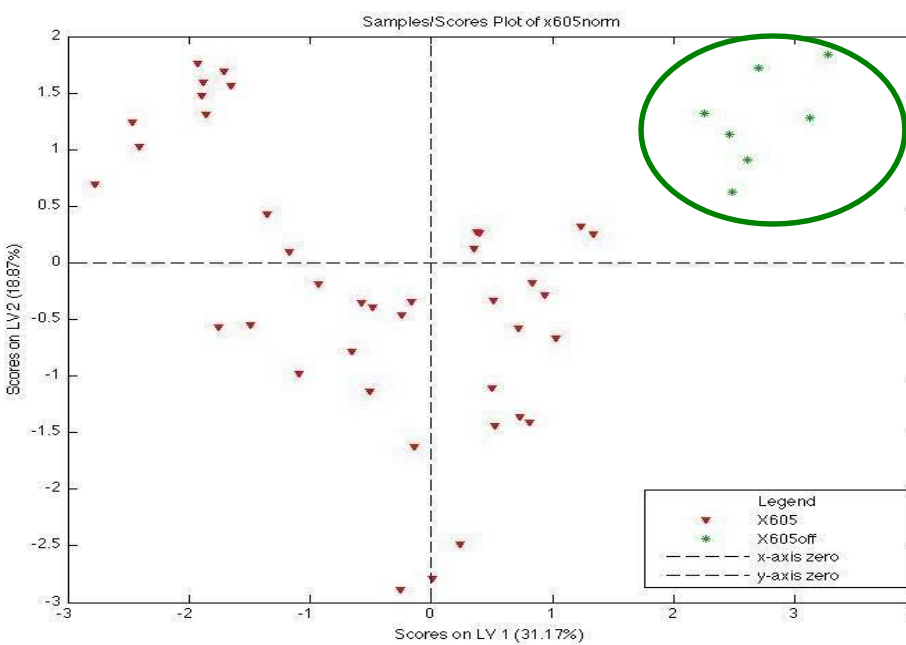
Real samples



Dark Chocolate



White Chocolate



Milk Chocolate

AuNP-Peptide vs. Porphyrin PLS-DA analysis

GNP-Peptide based

	Regular	Off	%
	Flavours	Correct	
Regular	48	0	100
Off flavours	0	7	100

Tot. Correct:

	Regular	Off	%
	Flavours	Correct	
Regular	39	0	100
Off flavours	0	7	100

Tot. Correct:

	Regular	Off	%
	Flavours	Correct	
Regular	51	1	98
Off flavours	0	7	100

Tot. Correct:

Porphyrin based

	Regular	Off	%
	Flavours	Correct	
Regular	14	1	93
Off flavours	1	9	90

Tot. Correct:

	Regular	Off	%
	Flavours	Correct	
Regular	13	1	92
Off flavours	4	8	67

Tot. Correct:

	Regular	Off	%
	Flavours	Correct	
Regular	15	1	94
Off flavours	4	8	67

Tot. Correct:

Virtual screening Peptides

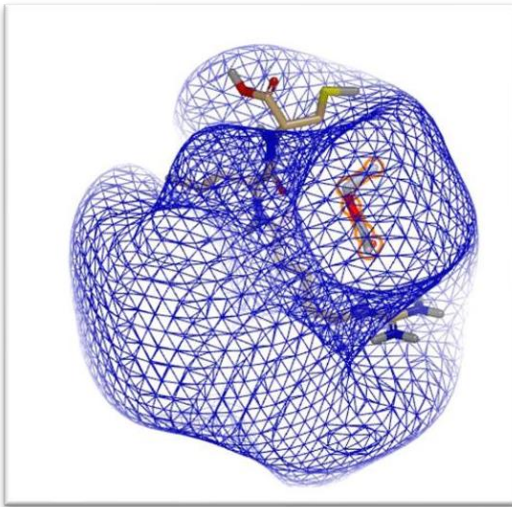
6 Peptides studied

(KSDSC, WHVSC, LGFDC, IHRIC,
LAWHC, TGKFC)

VS

14 volatile compounds

(different chemical classes, shapes,
dimensions, hydrophobicity)

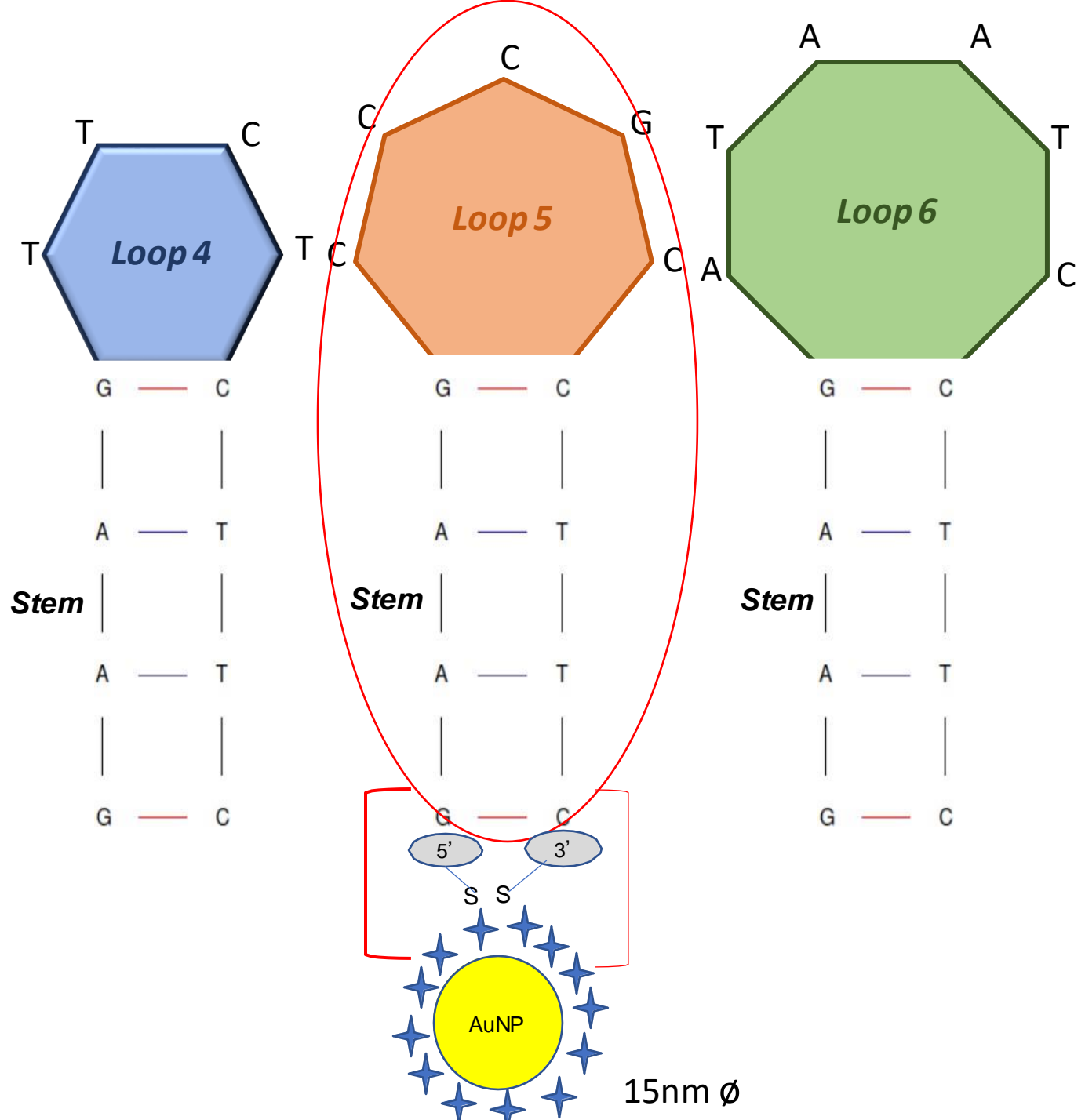


- Docking box generation 10 conformers for each peptide for identification of most probable bond sites and energy quantification involved in the docking simulation
- From 1 to 200 conformers for each volatile compound
- Binding score: average of all conformers

Hp-DNA

hpDNA has been used as molecular switch for optical and electrochemical sensing

- The loop can be used as sensing elements also for VOCs
- A virtual screening of the entire library sequences of the loops is possible
- hpDNA can be easily bound to metal nanoparticles (AuNPs)

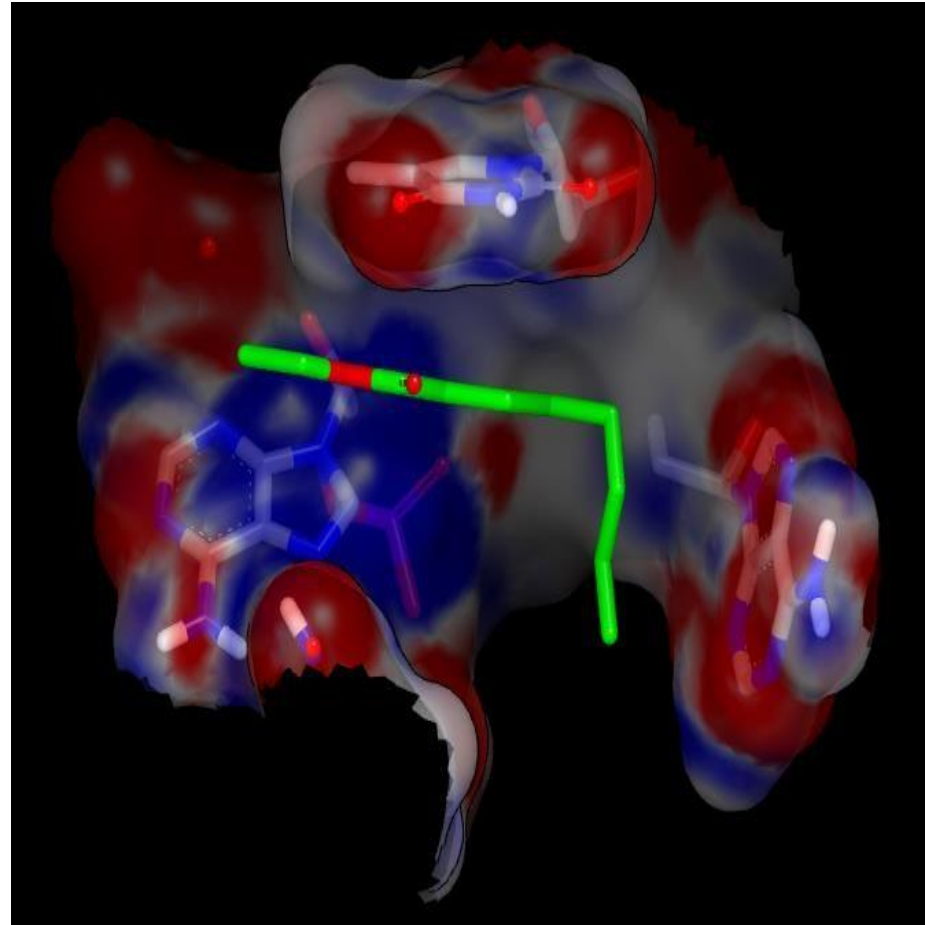


Virtual screening of hp-DNA

Virtual screening procedure was aimed to test the virtual binding affinities of the hairpin loop versus different chemical classes:



- Alcohols (14 molecules);
- Aldehydes (13 molecules);
- Esters (18 molecules);
- Ketones (5 molecules).

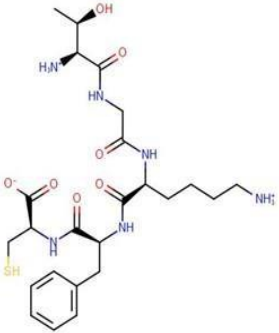


Molecular Modeling : octanal-ATAATC

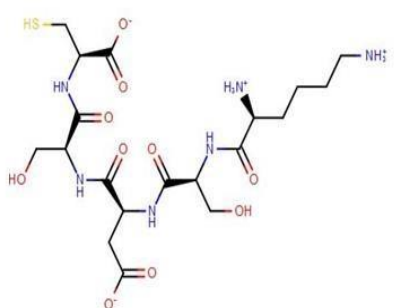
Electronic nose sequences...

n=20

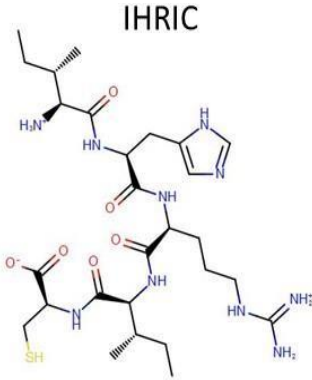
TGKFC



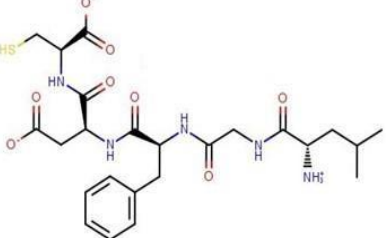
KSDSC



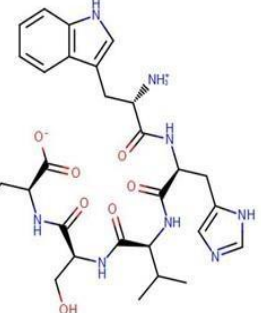
IHRIC



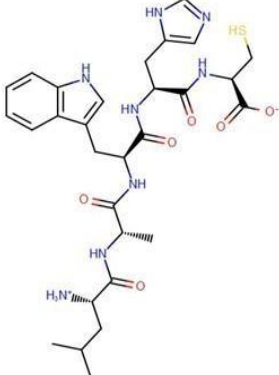
LGFDC



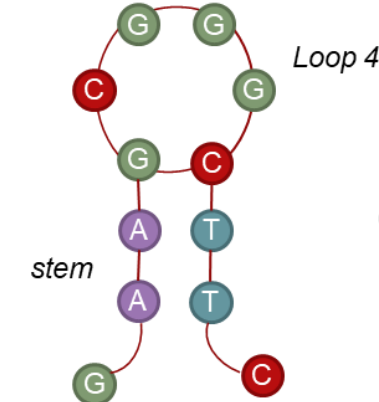
WHVSC



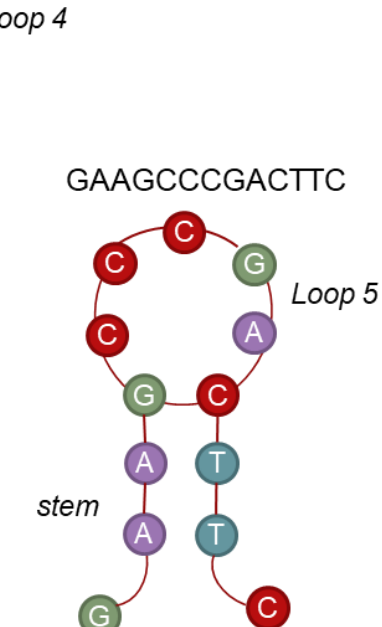
LAWHC



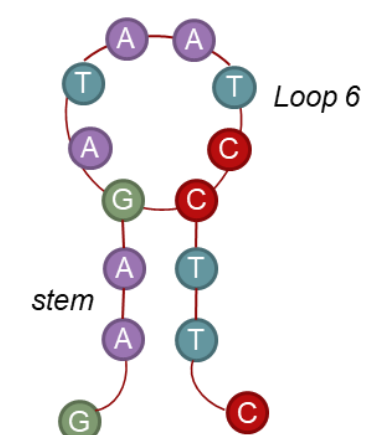
GAAGCGGGCTTC



GAAGCCCGACTTC

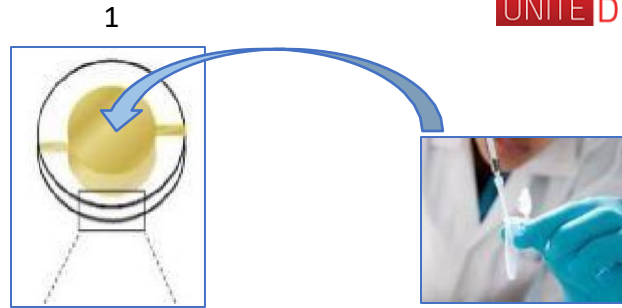


GAAGATAATCCTTC



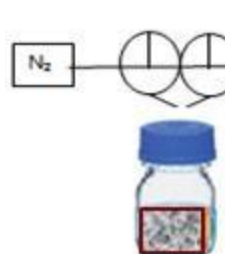
E-nose analysis

5 μ L of the AuNPs-hpDNA and ZnO-Peptide suspension on each side of the QCM



3

✓ Aroma release in headspace of gas-tight bottle

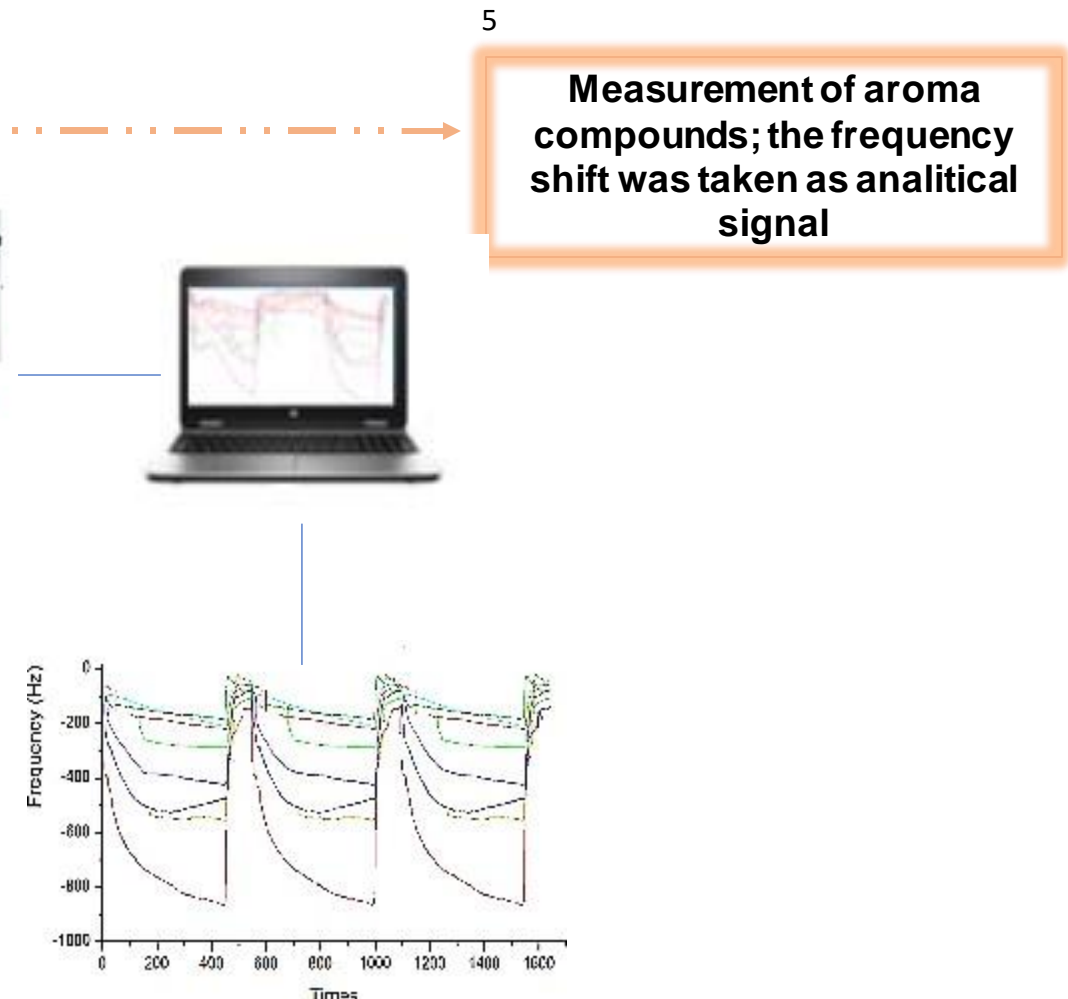


2

✓ The samples was introduced in a gas-tight bottle (100 mL)



4



5

Measurement of aroma compounds; the frequency shift was taken as analytical signal

SPME-GC/MS analysis

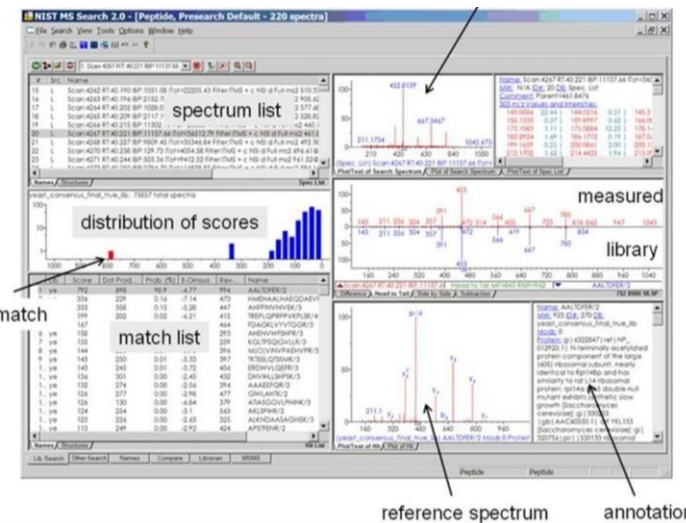
headspace
analysis



Desorption



Nistlibrary



Confirmed by Retention index..

Example...

Peak no.	RT ^{a)} (min)	RI _{lit} ^{b)}	RI _{cal} ^{c)}	Identification ^{d)}	Metabolite	MF ^{e)}	<i>m/z</i> ^{f)}	Similarity (%)	Peak area ($\times 10^6$ area units) \pm RSD (%)					
									DVB/CAR/PDMS ^{g)}	PDMS ^{g)}	CAR/PDMS ^{g)}	PDMS/DVB ^{g)}	PEG ^{g)}	PA
1	1.42	-	908	MS, RI	Isoprene	C ₅ H ₈	32, 67, 53	96	0.1 \pm 7.8	-	0.4 \pm 1.2	0.7 \pm 1.5	-	-
2	3.92	1007	1016	MS, RI, ST	α -Pinene	C ₁₀ H ₁₆	93, 77, 121	93	0.7 \pm 9.7	1.0 \pm 2.8	0.6 \pm 2.9	0.5 \pm 2.5	0.1 \pm 3.1	0.02 \pm 8.2
3	4.77	1075	1057	MS, RI	Camphene	C ₁₀ H ₁₆	93, 121, 41	94	0.04 \pm 8.7	0.2 \pm 9.5	0.1 \pm 8.5	0.3 \pm 3.2	0.01 \pm 5.5	-
4	5.73	1116	1107	MS, RI, ST	β -Pinene	C ₁₀ H ₁₆	93, 41, 69	91	2.4 \pm 1.2	5.8 \pm 3.9	3.0 \pm 3.2	3.2 \pm 8.0	0.5 \pm 2.7	0.1 \pm 1.3
5	8.79	1145	1135	MS, RI, ST	β -Myrcene	C ₁₀ H ₁₆	93, 69, 41	97	153.3 \pm 1.1	191.1 \pm 1.7	159.3 \pm 1.9	126.7 \pm 1.9	27.7 \pm 2.5	7.6 \pm 5.0
6	9.53	1180	1172	MS, RI, ST	Limonene	C ₁₀ H ₁₆	68, 93, 79	93	1.3 \pm 1.3	1.1 \pm 5.0	1.2 \pm 5.0	1.7 \pm 7.6	0.3 \pm 2.9	0.1 \pm 2.1
7	10.01	1185	1182	MS, RI	β -Phellandrene	C ₁₀ H ₁₆	93, 77, 136	95	1.1 \pm 2.6	0.2 \pm 6.8	0.9 \pm 5.1	1.1 \pm 1.0	-	-
8	11.64	1242	1246	MS, RI	<i>trans</i> - β -Ocimene	C ₁₀ H ₁₆	93, 79, 41	89	0.1 \pm 1.2	0.1 \pm 7.4	0.1 \pm 1.1	0.1 \pm 2.4	0.01 \pm 4.2	-
9	11.79	1262	1267	MS, RI, ST	α -Terpinene	C ₁₀ H ₁₆	93, 136, 77	91	0.1 \pm 1.4	0.1 \pm 3.3	0.1 \pm 2.6	0.1 \pm 2.7	0.01 \pm 3.5	-
10	12.48	1274	1279	MS, RI	<i>cis</i> - β -Ocimene	C ₁₀ H ₁₆	93, 76, 41	92	2.1 \pm 1.3	2.6 \pm 3.2	2.2 \pm 2.5	1.5 \pm 2.5	0.2 \pm 1.0	0.03 \pm 1.3
11	13.15	-	1290	MS, RI, ST	α -Cymene	C ₁₀ H ₁₆	119, 32, 134	95	0.1 \pm 1.9	0.1 \pm 2.7	0.1 \pm 1.3	0.04 \pm 1.3	0.01 \pm 1.2	-
12	13.75	1284	1280	MS, RI	α -Terpinolene	C ₁₀ H ₁₆	93, 121, 13	97	0.1 \pm 3.4	0.1 \pm 3.6	0.1 \pm 1.0	0.1 \pm 2.8	0.01 \pm 1.1	-
13	22.88	1295	1305	MS, RI	Perillene	C ₁₀ H ₁₆ O	69, 81, 150	96	0.2 \pm 1.5	0.2 \pm 8.6	0.2 \pm 2.9	0.2 \pm 2.5	0.03 \pm 2.3	-
14	26.07	1476	1481	MS, RI	Ylangene	C ₁₀ H ₁₆	105, 119, 161	95	0.4 \pm 2.0	0.2 \pm 5.8	0.3 \pm 2.0	0.2 \pm 3.2	-	-
15	26.64	1480	1491	MS, RI	α -Cubene	C ₁₀ H ₁₆	161, 119, 105	91	1.2 \pm 2.0	0.8 \pm 1.7	0.8 \pm 1.6	0.7 \pm 3.5	0.1 \pm 2.2	0.3 \pm 1.6
16	33.62	1663	1621	MS, RI, ST	α -Humulene	C ₁₀ H ₁₆	133, 93, 69	96	48.1 \pm 7.5	52.8 \pm 2.0	41.4 \pm 1.5	36.8 \pm 3.7	10.9 \pm 2.6	3.1 \pm 8.0
17	38.63	1657	1665	MS, RI, ST	β -Caryophyllene	C ₁₀ H ₁₆	93, 80, 121	93	42.4 \pm 4.1	21.3 \pm 2.3	16.8 \pm 1.9	15.4 \pm 3.6	3.6 \pm 2.5	1.0 \pm 2.2
18	39.90	1681	1687	MS, RI	γ -Muurolene	C ₁₀ H ₁₆	161, 105, 119	88	1.7 \pm 2.7	1.3 \pm 2.8	0.9 \pm 1.8	0.8 \pm 1.4	0.6 \pm 3.3	0.1 \pm 1.9
19	41.40	1566	1554	MS, RI	Methyl geranate	C ₁₀ H ₁₈ O ₂	69, 41, 114	90	3.7 \pm 1.1	3.1 \pm 4.2	1.3 \pm 3.1	2.3 \pm 2.0	0.4 \pm 2.8	0.1 \pm 3.2
20	41.89	1724	1713	MS, RI, ST	α -Selinene	C ₁₀ H ₁₆	189, 161, 93	92	0.8 \pm 9.8	0.2 \pm 2.3	0.2 \pm 6.8	0.4 \pm 4.1	0.2 \pm 3.0	0.04 \pm 2.3
21	42.50	-	1744	MS, RI	α -Murolene	C ₁₀ H ₁₆	105, 161, 93	89	0.3 \pm 2.5	0.3 \pm 1.8	0.2 \pm 1.6	0.2 \pm 4.1	0.1 \pm 3.6	0.02 \pm 1.4
22	44.59	1749	1740	MS, RI, ST	(+)- δ -Cadinene	C ₁₀ H ₁₆	161, 134, 119	89	1.9 \pm 2.2	1.6 \pm 1.8	1.0 \pm 1.5	1.0 \pm 4.2	0.4 \pm 2.6	0.1 \pm 1.0
23	45.88	-	1755	MS, RI, ST	Cubenene	C ₁₀ H ₁₆	119, 105, 161	93	0.3 \pm 5.4	0.2 \pm 5.7	0.1 \pm 1.2	0.2 \pm 4.4	0.1 \pm 3.8	0.01 \pm 7.1
24	46.60	-	1769	MS, RI	Naphthalene H ₄ 7DM 1R ^{h)}	C ₁₀ H ₁₆	105, 161, 91	96	0.2 \pm 2.5	0.1 \pm 2.1	0.1 \pm 2.0	0.1 \pm 4.7	0.1 \pm 6.3	0.01 \pm 9.8
25	48.27	-	1780	MS, RI	β -Fenchene	C ₁₀ H ₁₆	79, 32, 67	95	0.1 \pm 3.0	0.1 \pm 4.6	0.02 \pm 2.7	0.04 \pm 5.2	0.01 \pm 1.1	0.01 \pm 1.0
26	49.30	1800	1789	MS, RI, ST	3-Carene	C ₁₀ H ₁₆	69, 93, 41	98	0.9 \pm 2.5	0.4 \pm 1.1	0.3 \pm 2.3	0.4 \pm 5.0	0.3 \pm 1.2	0.04 \pm 8.0
27	51.68	1825	1835	MS, RI, ST	cis-Geraniol	C ₁₀ H ₁₈ O	69, 41, 93	92	0.2 \pm 2.0	0.1 \pm 3.9	0.1 \pm 3.2	0.1 \pm 2.0	0.1 \pm 1.0	-
						Total peak area ($\times 10^6$)		263.7	285.0		231.8	194.4		45.6 \pm 12.4
						Average RSD (%)		3.4	3.9		2.7	3.4		2.8 \pm 3.9
						No. metabolite by fiber		27	26		27	24		17

a) Retention time (min).
b) Kovat's retention index reported in the literature for BP-20 capillary column or equivalents [53].
c) Kovat's retention index relative n-alkanes(C₆-C₂₀) on a BP-20 capillary column.

Headspace Volatile Evaluation of Carrot Samples Comparison of GC/MS and AuNPs-hpDNA-Based E-Nose



- Monitoring and control of vegetable ripening are important parameters in the food industry, since the maturation state during harvest, storage and distribution on the market defines the quality of the finished product;
- To prevent enzymatic reactions during processing, storage and thawing, the packaged carrots were blanched at 95 °C for 8 min in a water bath
- 3 g of blanched carrots were placed in 20 ml gas-tight vials and hermetically sealed with a gas-tight septum. A total of 24 vials were prepared for each temperature tested (-18 °C, 4 °C, 25 °C, 40 °C), in order to have three replicates (three different vials) for each day of measurement (1, 4, 8, 12, 19, 26 days). Thus, a total of 140 vials for E-nose and GC-MS have been analyzed. Each vial was used only once for either the GC-MS or E-nose measurement and the relative sample was discarded.

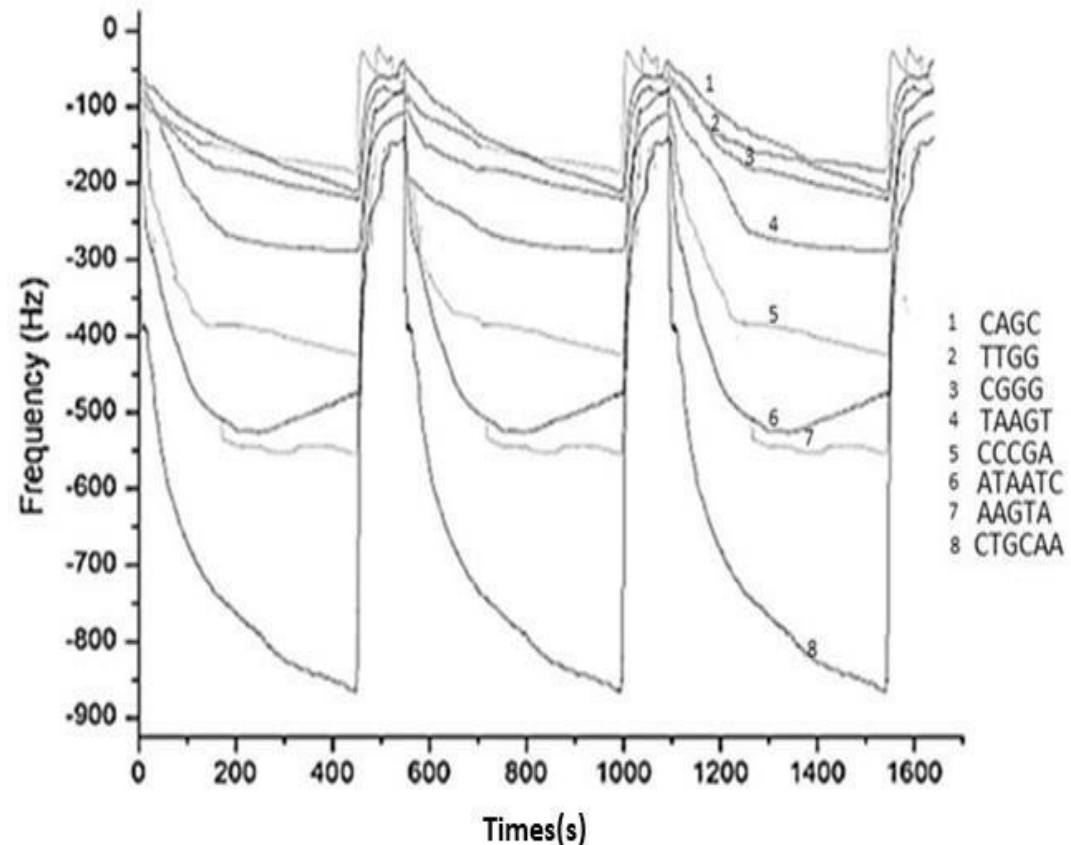
Volatile compounds	GC area (%)																				
	Storage time (days)																				
	-18 °C					4 °C					25 °C					40 °C					
	1	4	8	12	19	1	4	8	12	19	26	1	4	8	12	19	26	1	4	8	12
α-phellandrene	n.d.	n.d.	n.d.	n.d.	n.d.	1	1	1	1	1	n.d.	n.d.**	1	n.d.	n.d.	1	n.d.	7	1	n.d.	n.d.
β-phellandrene	2	1	2	1	1	3	3	2	1	4	1	n.d.	3	1	1	2	n.d.	n.d.	n.d.	n.d.	n.d.
terpinolene	n.d.	n.d.	1	1	0	1	1	1	n.d.	1	n.d.	n.d.	1	n.d.	n.d.	1	n.d.	n.d.	n.d.	n.d.	n.d.
α-pinene	14	9	12	12	10	14	12	14	14	18	8	12	7	12	11	15	2	n.d.	10	15	5
(-) β-pinene	3	2	3	3	3	3	3	3	3	3	2	2	3	2	2	3	1	n.d.	n.d.	n.d.	2
β-pinene	3	2	3	2	6	5	6	3	3	5	1	2	6	1	1	4	n.d.	5	3	3	2
Octanal	1	1	n.d.	n.d.	n.d.	1	1	1	1	n.d.	n.d.	1	n.d.	n.d.	n.d.	n.d.	n.d.	n.d.	n.d.	n.d.	n.d.
γ-terpinene	7	8	9	10	7	8	9	7	8	4	1	12	7	6	5	7	n.d.	21	9	9	5
β-farnesene	1	1	1	1	1	1	1	1	1	n.d.	1	1	1	1	1	1	2	n.d.	n.d.	n.d.	n.d.
α-caryophyllene	1	1	1	1	2	2	1	1	1	1	5	1	2	1	2	1	2	n.d.	n.d.	n.d.	n.d.
β-copaene	2	2	2	n.d.	4	2	2	3	n.d.	n.d.	n.d.	2	1	2	2	2	5	n.d.	n.d.	n.d.	n.d.
myristicin	1	1	1	1	2	1	1	1	1	1	5	2	1	2	n.d.	1	4	n.d.	n.d.	n.d.	n.d.
elemicin	n.d.	1	n.d.	n.d.	n.d.	n.d.	n.d.	1	n.d.	n.d.	4	1	n.d.	1	1	n.d.	2	n.d.	n.d.	n.d.	n.d.
butane-2,3-diol	n.d.	n.d.	n.d.	n.d.	n.d.	n.d.	n.d.	n.d.	n.d.	n.d.	n.d.	n.d.	n.d.	2	2	5	13	n.d.	n.d.	n.d.	3
acetoin	n.d.	n.d.	n.d.	n.d.	n.d.	n.d.	n.d.	n.d.	n.d.	n.d.	n.d.	n.d.	n.d.	9	3	6	15	5	3	5	6
ethanol	n.d.	n.d.	n.d.	n.d.	n.d.	n.d.	n.d.	n.d.	n.d.	n.d.	n.d.	n.d.	n.d.	n.d.	n.d.	n.d.	n.d.	5	n.d.	n.d.	6
lactamide	n.d.	n.d.	n.d.	n.d.	n.d.	n.d.	n.d.	n.d.	n.d.	n.d.	n.d.	n.d.	n.d.	n.d.	n.d.	n.d.	n.d.	4	11	16	7
3-methylbutan-1-ol	n.d.	n.d.	n.d.	n.d.	n.d.	n.d.	n.d.	n.d.	n.d.	n.d.	n.d.	n.d.	n.d.	n.d.	n.d.	1	2	1	3	3	3

*(mean value of n=3 repetitions); **n.d.: not detected.

Results of the gas-chromatographic (GC) analysis of the headspace of carrots samples. Data are expressed as % of the total GC area*.

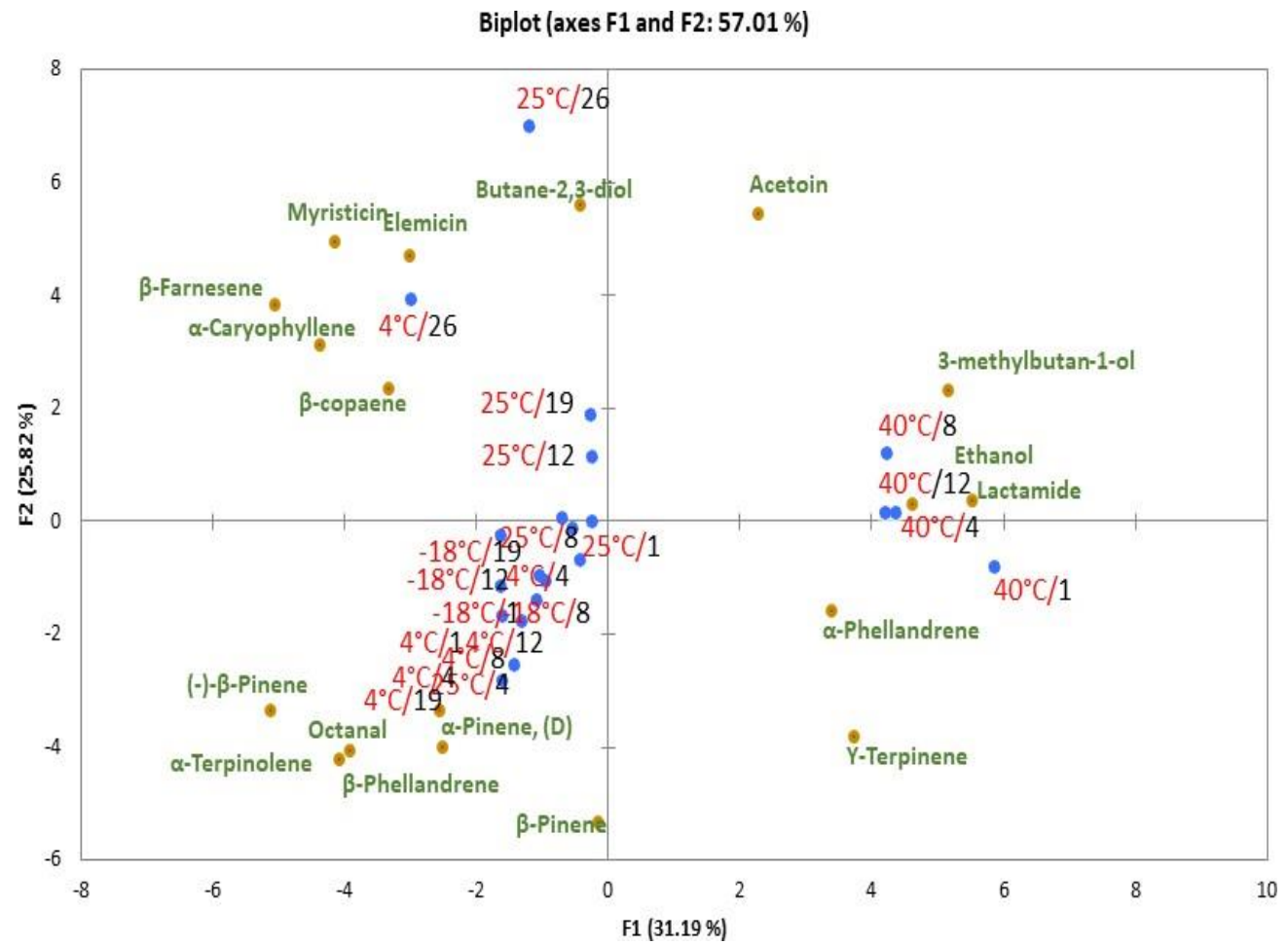
Carrots Sample	CGGG	TTGG	CTGCAA	CAGC	TAAGT	AAGTA	ATAATC	CCCGA
25°C/1	145	199	314	187	409	566	686	147
4°C/1	118	221	132	155	417	468	564	107
-18°C/1	111	241	199	150	415	485	529	127
25°C/4	103	259	323	164	495	575	645	146
4°C/4	107	230	317	159	535	492	608	156
-18°C/4	101	208	244	155	577	513	603	165
25°C/8	148	228	339	237	544	462	787	216
4°C/8	130	204	179	174	480	632	701	180
-18°C/8	129	188	197	140	498	493	603	175
25°C/12	127	201	311	182	529	564	716	192
4°C/12	126	180	414	147	470	553	660	141
-18°C/12	105	205	403	166	602	495	664	148
25°C/19	87	131	120	100	374	515	565	135
4°C/19	86	257	301	145	483	696	600	160
-18°C/19	114	224	307	118	421	662	607	150
25°C/26	46	88	289	161	146	583	494	140
4°C/26	64	118	370	101	358	497	576	145
40°C/1	41	98	250	176	169	468	755	175
40°C/3	51	146	252	192	160	507	733	214
40°C/4	53	143	235	194	168	507	693	167
40°C/9	45	217	263	150	239	453	686	168

Frequency shift (Hz) response of the HpDNA sensors array for the carrots samples. The coefficient of variation calculated using three measurements taken in three different days was in all cases below 15%.



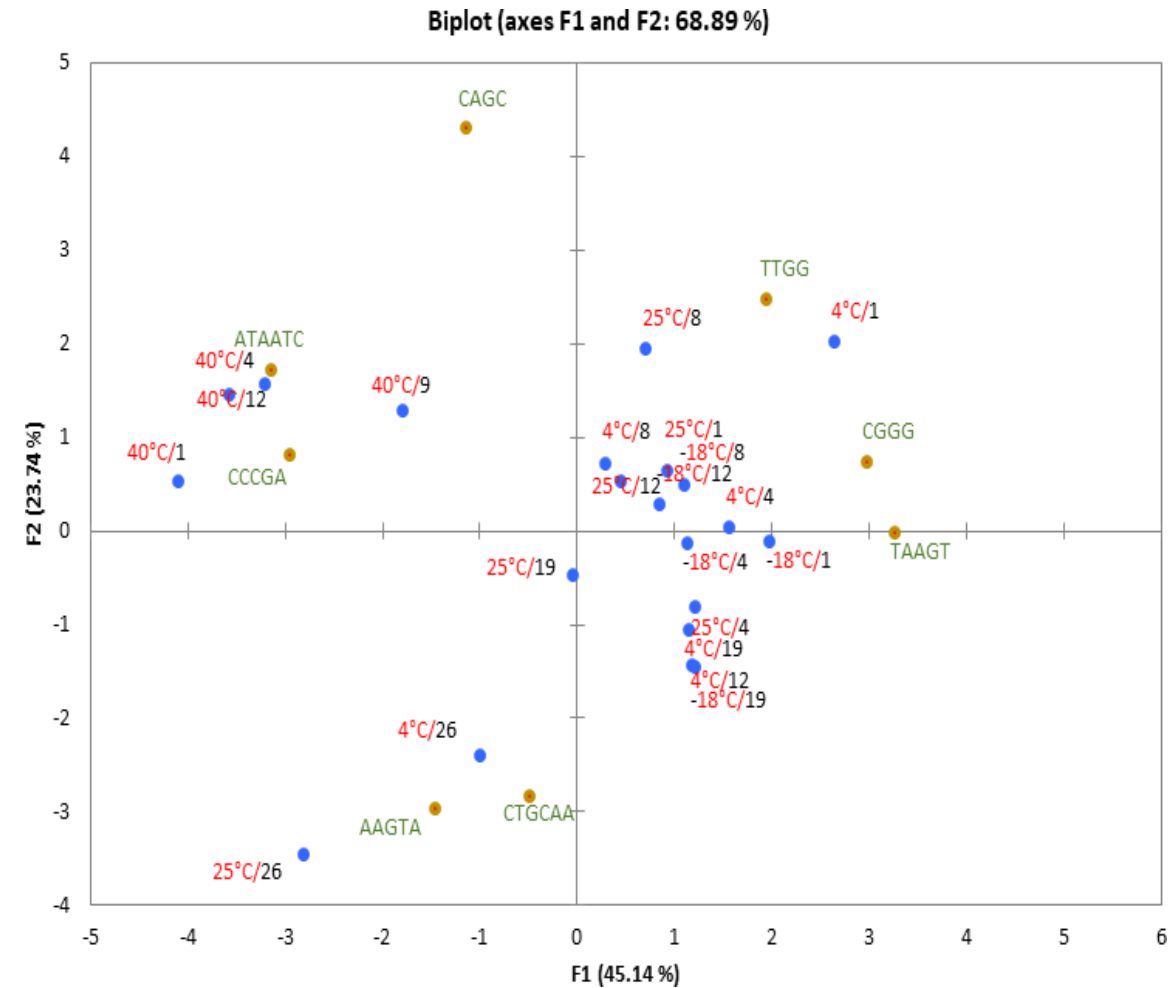
Frequency signal recorded with AuNPs-hpDNA testing carrots samples in triplicate

GC-MS



PCA of the GC-MS/SPME response of carrot samples stored for different time at various temperature. Data are expressed in (Relative Abundance %) before PCA

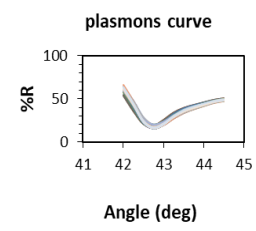
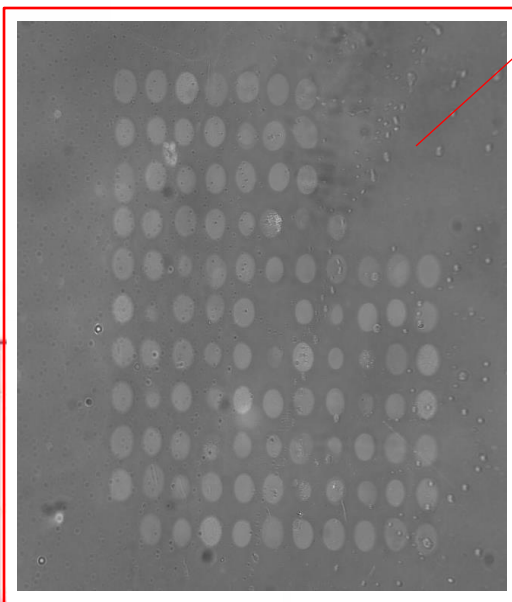
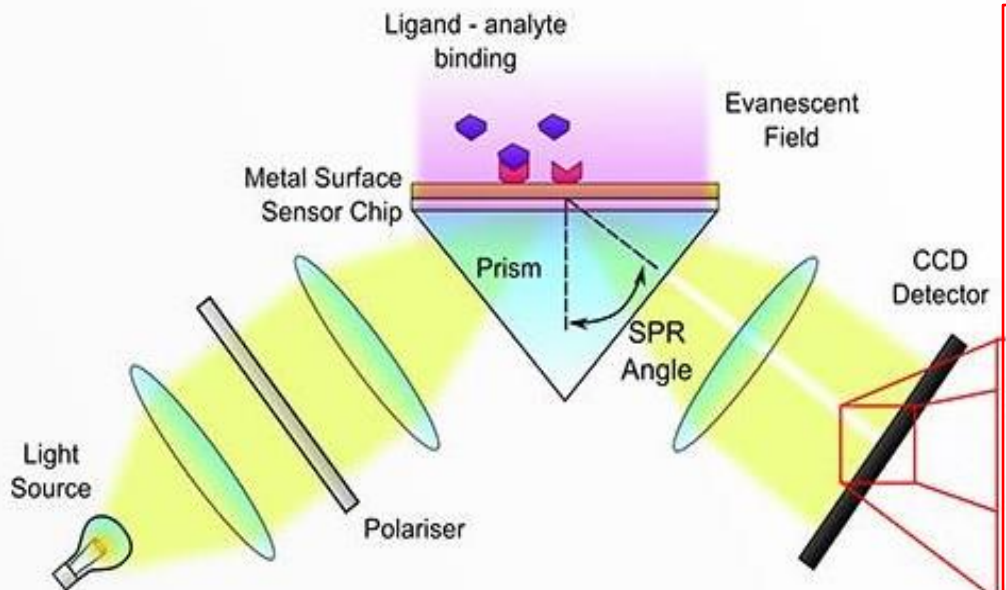
E-nose



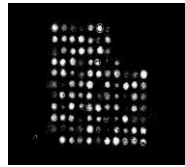
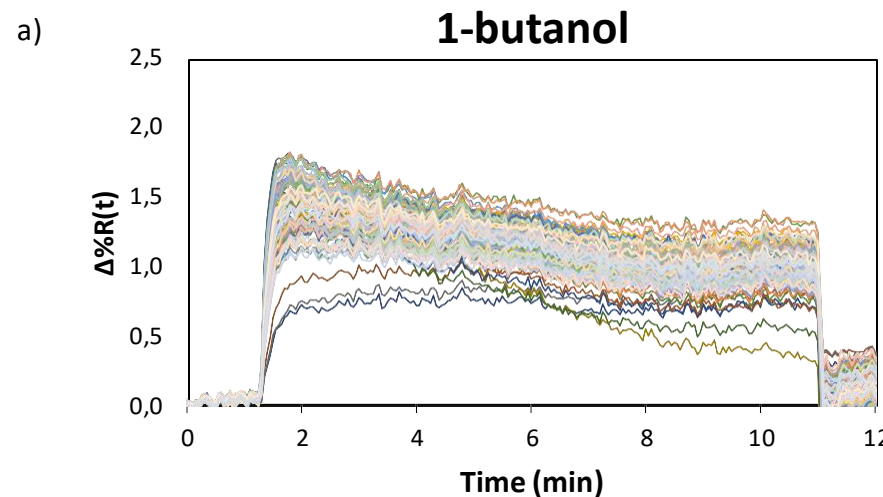
PCA biplot (scores and loadings) of the E-nose response to carrots samples. Data were normalized before PCA

Surface plasmon resonance imaging

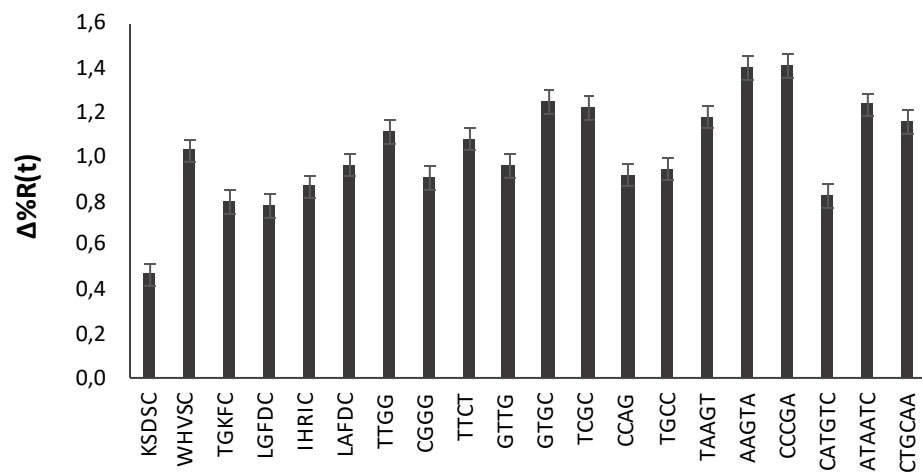
home-made SPRI system



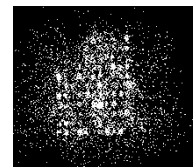
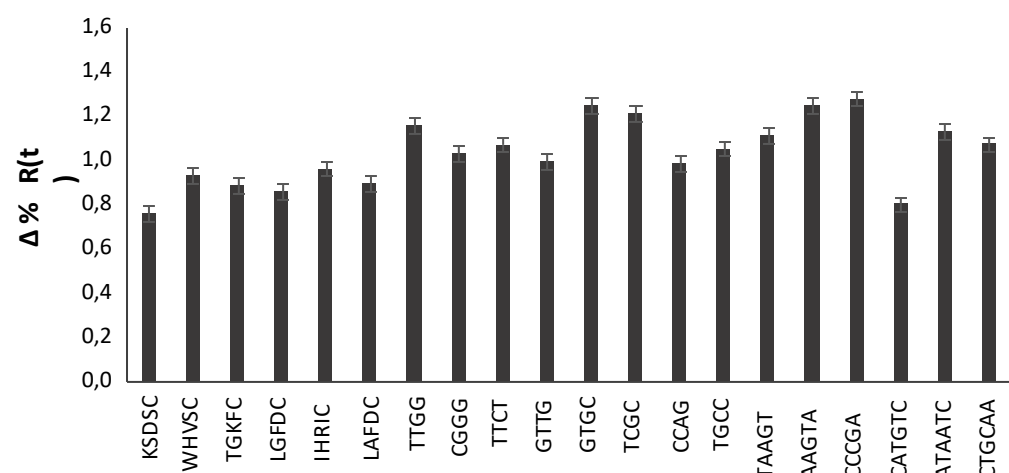
- 104 spot
- 12 peptides at different concentration: 200 μ M and 400 μ M
- 14 hpDNA: 16.8 μ M
- 1.2 nL volume drop (\leq 1mm)



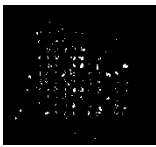
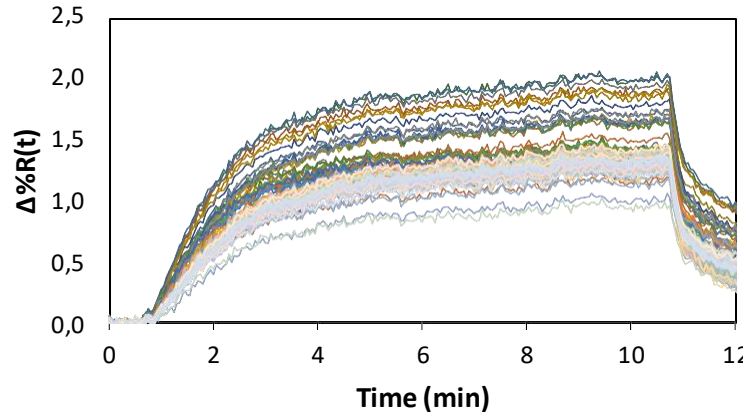
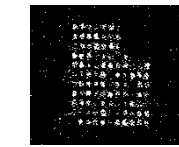
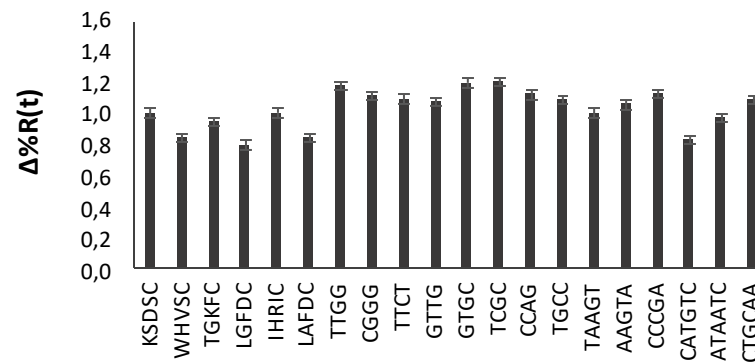
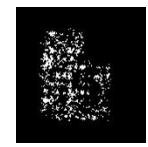
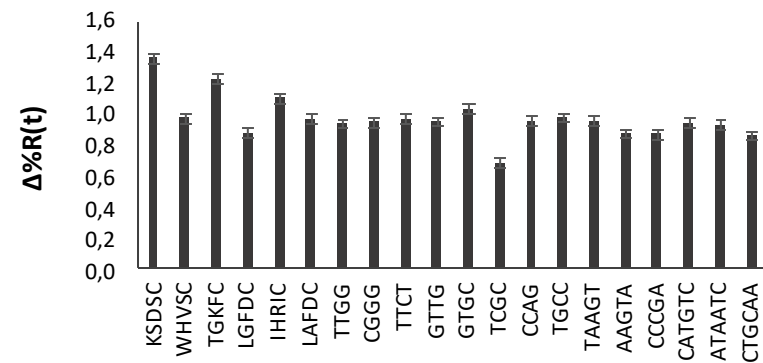
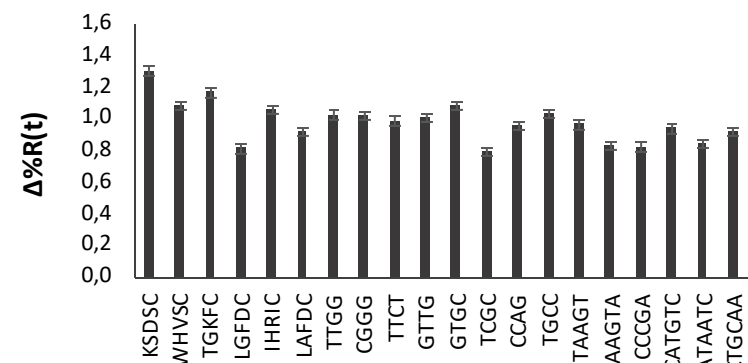
1-butanol

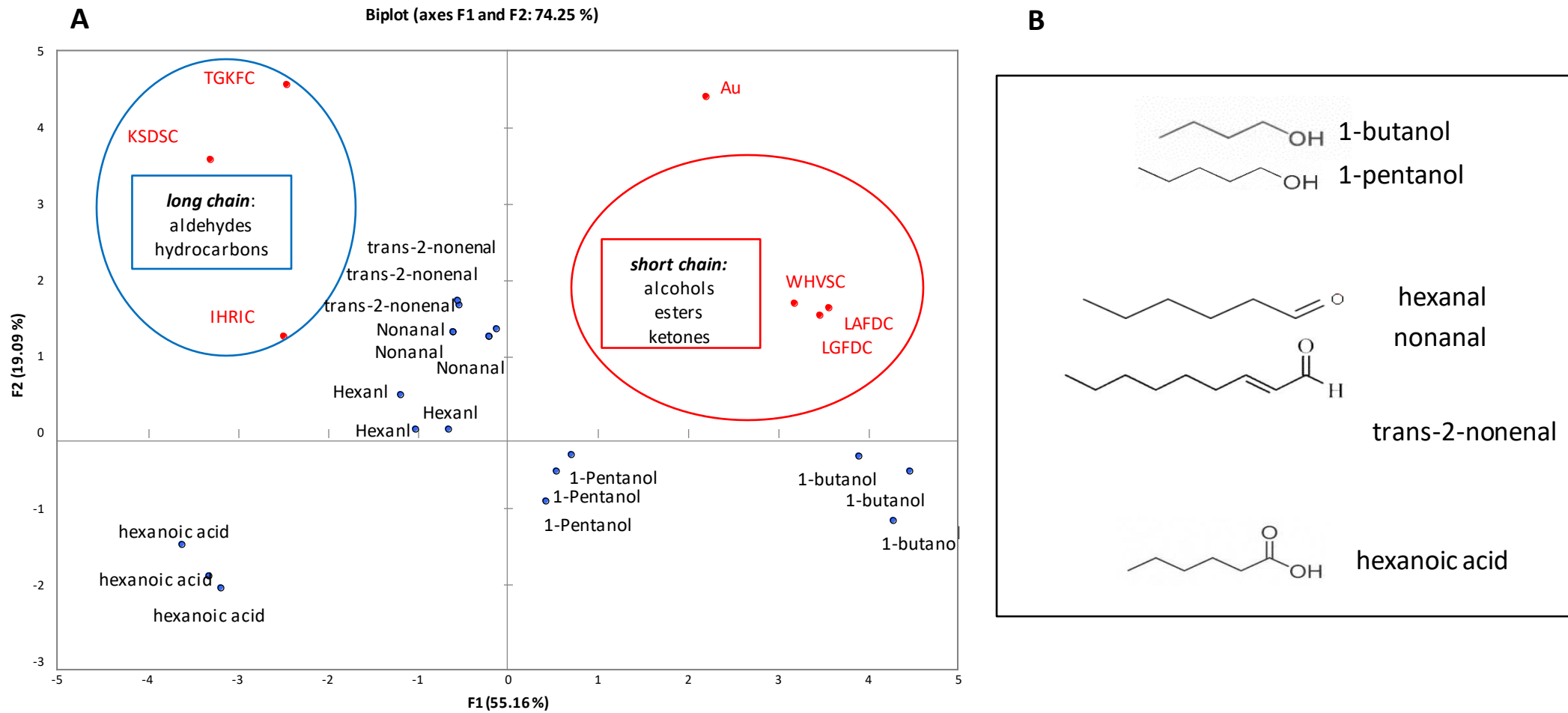


1-pentanol

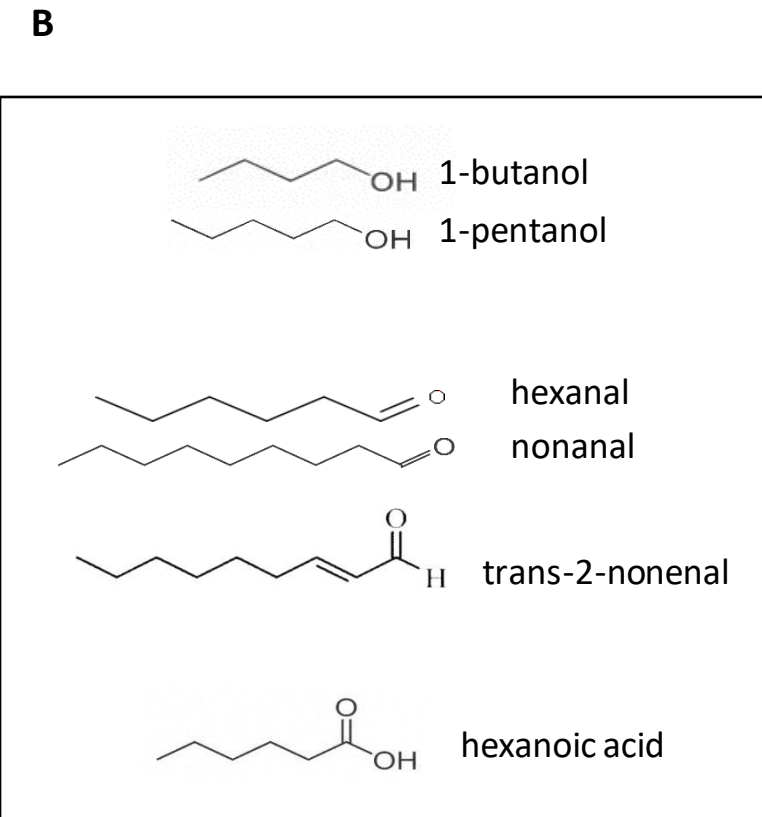
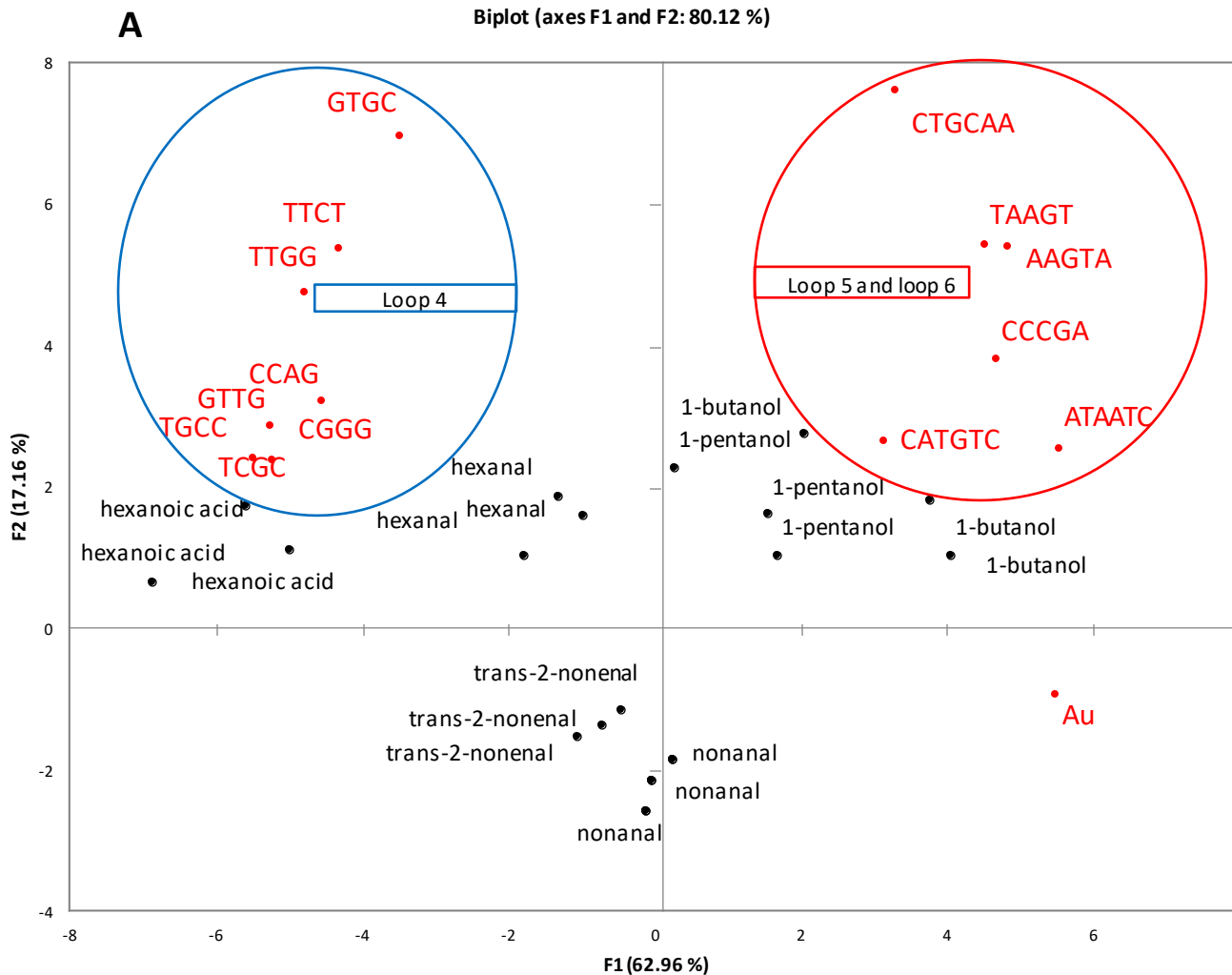


b)

nonanal**hexanal****nonanal****trans-2-nonenal**



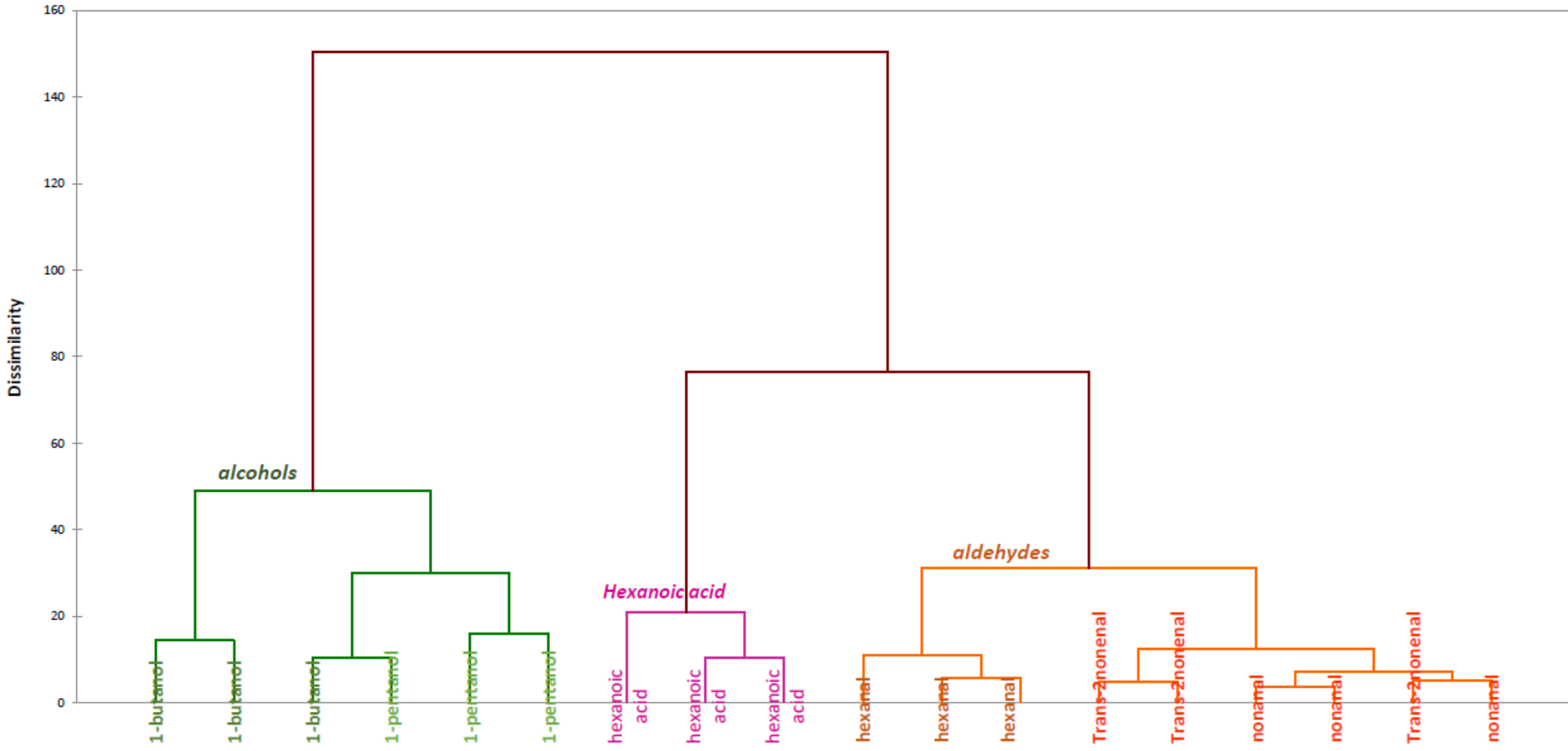
(A) PCA (*loading* and *score* plots) for the discrimination of different VOCs with different penta-peptides; (B) Explain the different chemical structures of VOCs tested: 1-butanol, 1-pentanol, hexanal, trans-2-nonenal, hexanoic acid



(A) PCA(*loading and score plots*) for the discrimination of different VOCs with different hpDNA; (B) Explain the different chemical structures of VOCs tested: 1-butanol, 1-pentanol, hexanal, trans-2-nonenal, hexanoic acid

Agglomerative hierarchical Clustering (AHC) analysis with peptide and hpDNA

Dendrogram



Article

A Study of Diagnostic Accuracy Using a Chemical Sensor Array and a Machine Learning Technique to Detect Lung Cancer

Chi-Hsiang Huang ^{1,2}, Chian Zeng ³, Yi-Chia Wang ^{1,2}, Hsin-Yi Peng ³, Chia-Sheng Lin ⁴,
Che-Jui Chang ^{3,5}  and Hsiao-Yu Yang ^{3,6,*} 

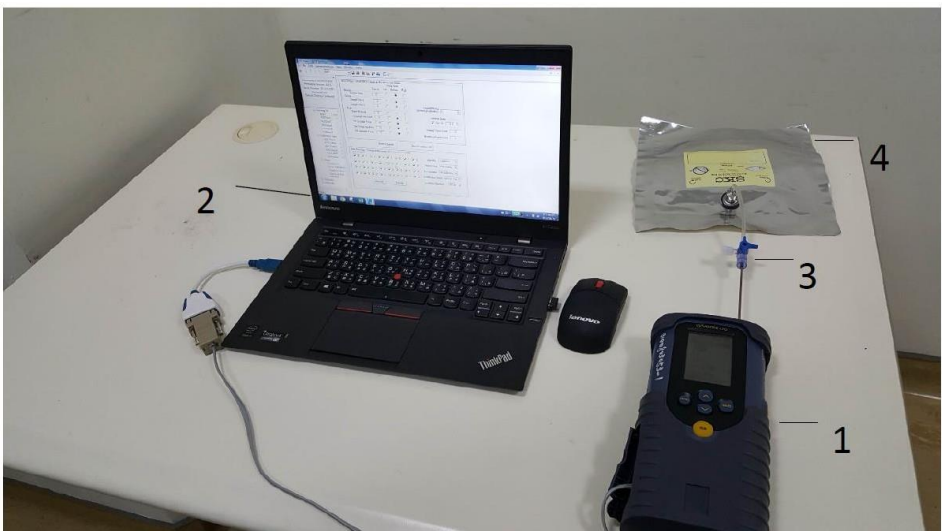


Figure S1. Experimental setup for the analysis of alveolar air consisting of a (1) E-nose, (2) computer, (3) three-way valve and (4) Tedlar bag.

Legend: The bags were connected with the necessary fixture, including an airtight PVC tube and a three-way valve for connection to the E-nose.

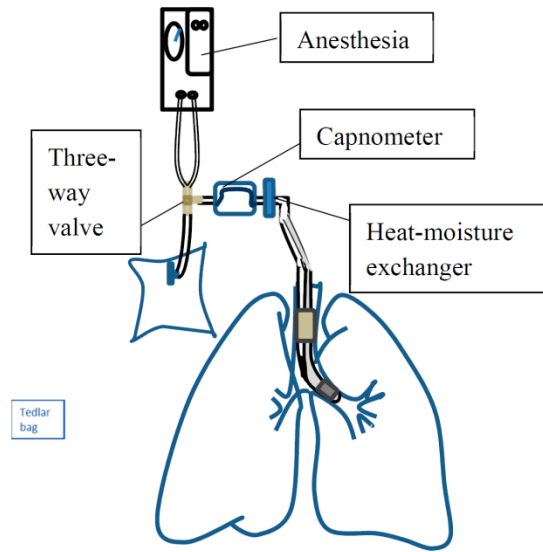


Figure 1. Schematic of the system framework and sample collection.

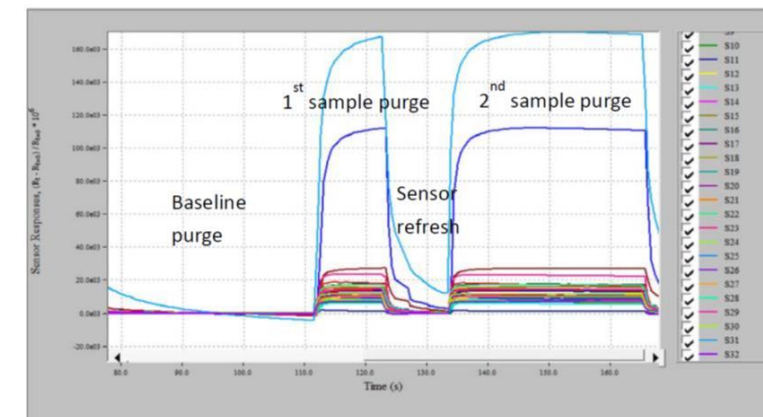


Figure S2. Desired waveforms for Cyranose320.

Legend: The setting comprised 10 seconds of a baseline purge and 40 seconds of a sample purge, which was sufficient for most sensors to reach the steady-state, followed by 10 seconds of a wash-out to return to the baseline.

Early detection of lung cancer with good specificity

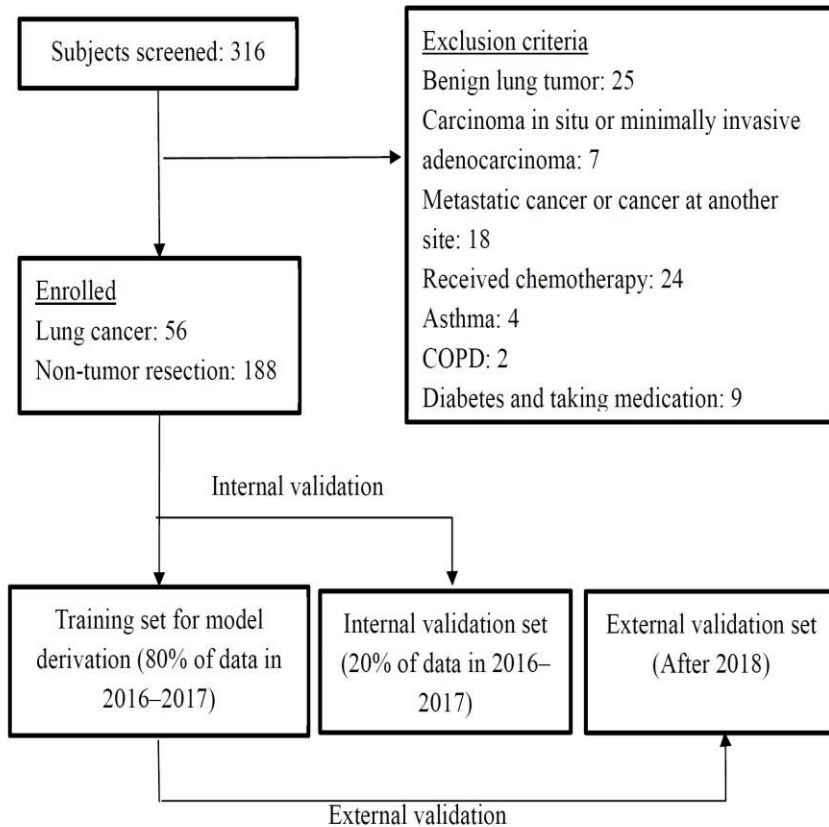


Figure 2. Flow diagram depicting the inclusion and exclusion of the study subjects. We employed an independent external validation set and conducted a repeated double cross-validation. The repeated double cross-validation used two nested loops. The inner loop used the study subjects enrolled between 2016 and 2017 as a calibration set for model selection and parameter optimization and were divided into a training set (80%) and an internal validation set (20%). The outer loop used the prediction model established from the calibration set to externally validate the study subjects enrolled in 2018.

Model	Sensitivity	Specificity	PPV	NPV	FP	FN	Accuracy
LDA internal validation	100.0%	88.6%	60.0%	100.0%	12.4%	0.0%	90.2%
LDA external validation	75.0%	96.6%	90.0%	90.3%	3.4%	25.0%	85.4%
SVM internal validation	92.3%	92.9%	85.7%	96.3%	7.1%	7.7%	92.7%
SVM external validation	83.3%	86.2%	71.4%	92.6%	13.8%	16.7%	85.4%

LDA, linear discriminant analysis; SVM, support vector machine; PPV, positive prediction rate; NPV, negative prediction value; FP, false-positive; FN, false-negative.

Non-invasive Detection of Bladder Tumors Through Volatile Organic Compounds: A Pilot Study with an Electronic Nose

HENDRIK HEERS¹, JOSEF MAXIMILIAN GUT¹, AXEL HEGELE¹, RAINER HOFMANN¹,
TOBIAS BOESELT², AKIRA HATTESOHIL² and ANDREAS REMBERT KOCZULLA²

¹Department of Urology and Paediatric Urology,
Philipps-Universität Marburg, Marburg, Germany;

²Department of Pulmonology, Philipps-Universität Marburg, Marburg, Germany

Urine samples, standard protocol for
bladder tumour diagnosis, cystoscopy

Table I. Patient demographics.

	Tumor	Control
Number of individuals	30	30
Mean age [years]	71.3	56.4
Age range [years]	49-86	21-85
Gender (male:female)	24:6	21:9
Smokers	6	6
Former smokers	8	1
Microscopic haematuria	17	7

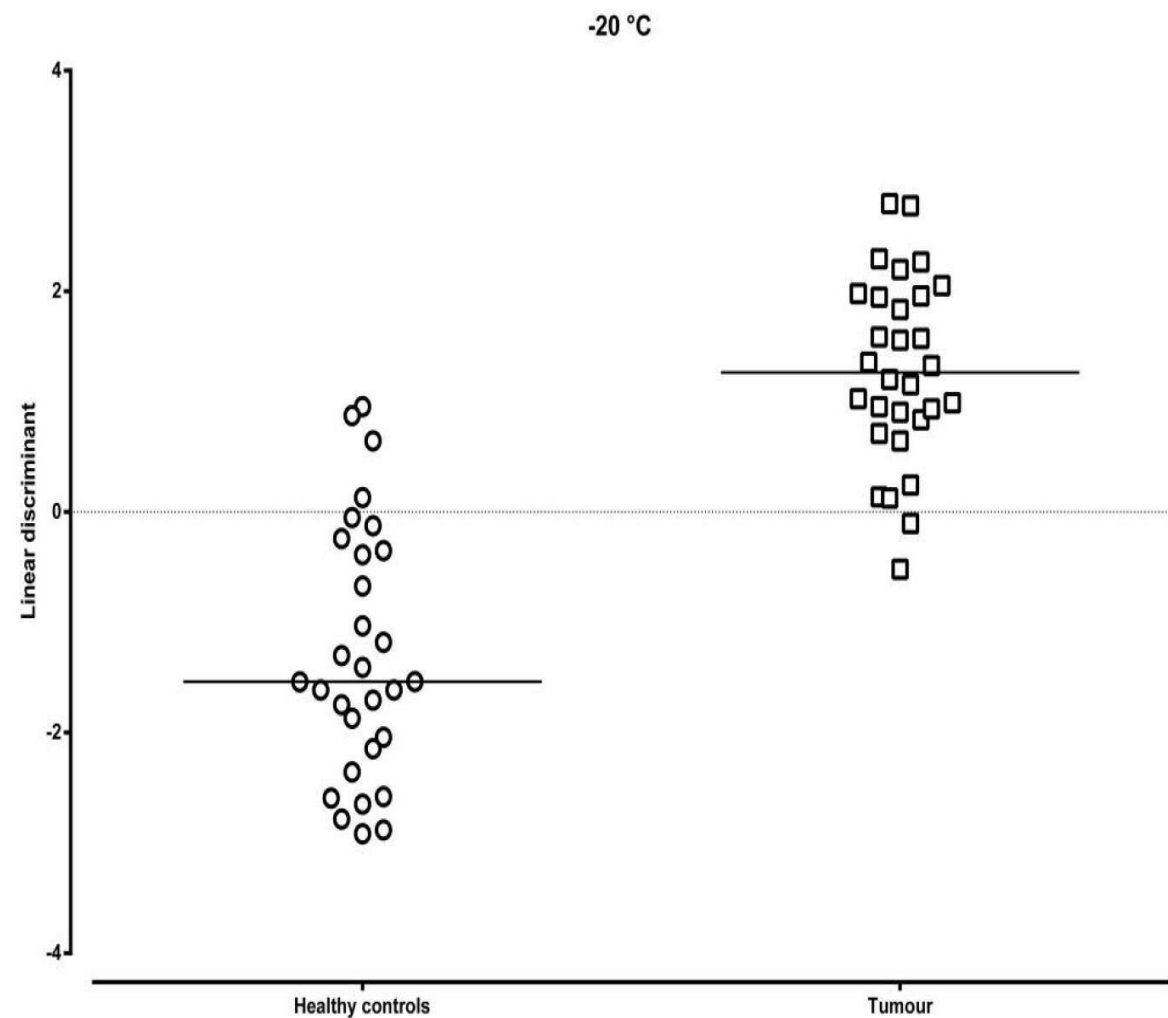
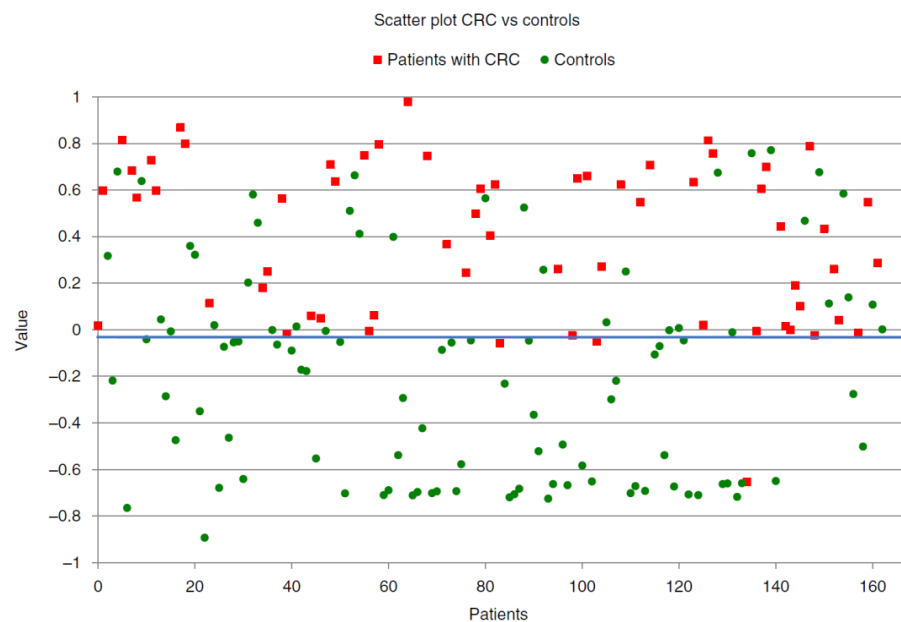


Figure 1. LDA for samples stored at -20°C.

Volatile organic compounds in breath can serve as a non-invasive diagnostic biomarker for the detection of advanced adenomas and colorectal cancer

Kelly E. van Keulen¹  | Maud E. Jansen^{2,3} | Ruud W. M. Schrauwen⁴ |
Jeroen J. Kolkman^{2,3}  | Peter D. Siersema¹ 



336



FIGURE 1 Electronic nose used in the study; the Aeonose (The eNose Company). Patients inhale through a carbon filter to prevent the entry of nonfiltered environmental air and breathe into the device through a disposable mouthpiece while wearing a nose clip

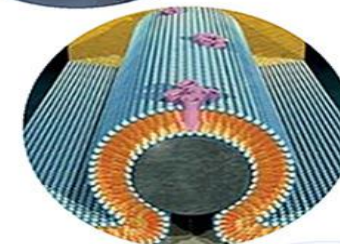
[Go to Biosensors and Bioelectronics on ScienceDirect](#)

Bioelectronic tongue: Current status and perspectives

Tomasz Wasilewski ^a   , Wojciech Kamysz ^a , Jacek Gębicki ^b



- BIOMIMETIC SENSORS



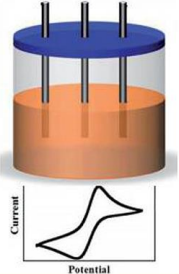
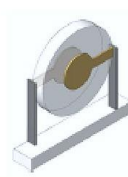
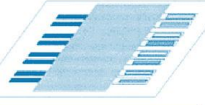
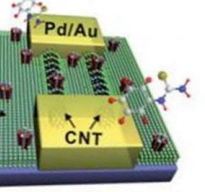
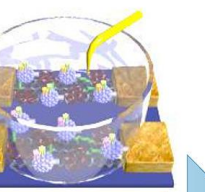
- MICRO/NANO TECHNOLOGIES

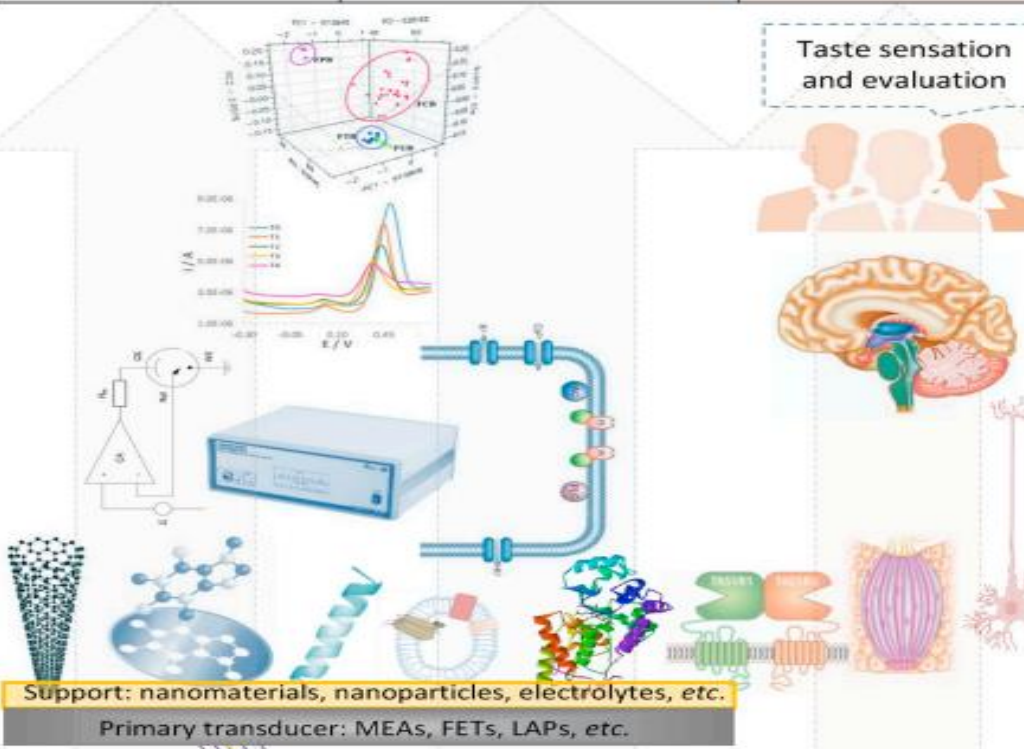


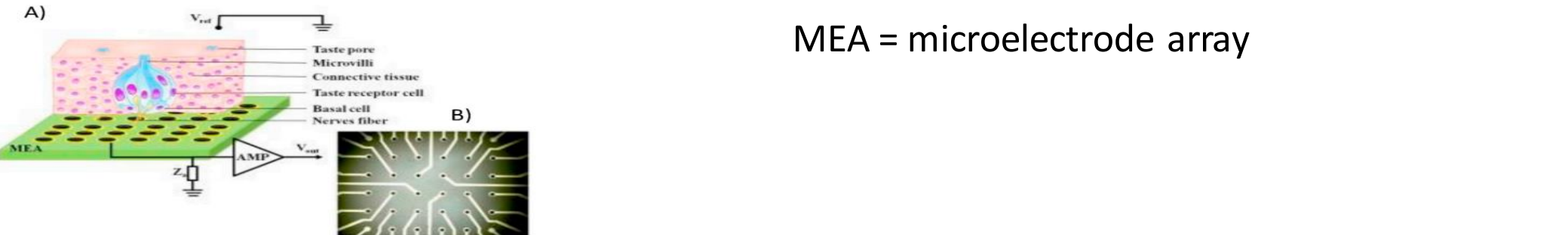
- APPLICATIONS



- PERSPECTIVES

									
1906-1937 pH glass electrode (GE) and ion-exchange theories, widely used for the description of behavior not only of GEs but also of other ion-selective electrodes.	1961-1969 Conventional ion-selective electrodes and biosensors. Starting point of modern potentiometry and selective response detection in biological membranes.	1970 → Microelectronics in sensor development, first ISFET and piezoelectric biosensor. First miniaturized sensors/biosensors capable to measure different parameters.	1985 → Multisensor arrays and sensor systems (Otto, Thomas). Rapid progress of semiconductor micromachining as the basis for integration into arrays. New trends in the biosensors technology, named micro total analytical systems (μ TAS) or the lab-on-a-chip.	1996 “Taste” sensor (Toko). Concept different from conventional chemical sensors, troughs a new light on food and environmental samples analysis techniques.	1998 First electronic tongue (Vlasov, Legin, D’Amico, Di Natale). Promising device in quantitative and qualitative analysis of multispecies solutions.	1999 Encoding taste receptors (Hoon <i>et al.</i>). Expansion knowledge of intracellular signaling pathways involved in taste transduction and critical steps in a comprehensive dissection of taste biology.	1999 First bioelectronic tongue (Bachmann, Schmid). Sensitive screen-printed amperometric multielectrode biosensor with Artificial Neural Network (ANN) employed for the rapid discrimination of the insecticides.	2010 Human-like nano-bioelectronic super-taster (Kim <i>et al.</i>) for detection of bitter tastants and distinguish between bitter and non-bitter tastants with similar chemical structures similarly to human tongue.	2016 Duplex bioelectronic tongue (Ahn <i>et al.</i>) expected to replace previous sensory evaluation strategies for the food and beverage industry and facilitate the functional study of dimeric GPCRs.

ELECTRONIC TONGUE	BIOELECTRONIC TONGUE	HUMAN TASTE
Results visualization and classification by chemometric tools to discriminate, identify or quantify the sample.		
Chemical/biological signals recording and data acquisition obtained from sensors/biosensors array and initial data analysis. Conversion of biological signals.		Taste sensation and evaluation
Sample analysis by sensors/biosensors array consist of primary transducers, supporting materials and secondary transducers (biosensing element in case of B-ET).		
Sample transfer through pumps/valves, microfluidic systems.		
Sampling system, optional step of sample collection.		
		Qualitative and hedonic sensations are perceived. Through synapse and neurons an electrical impulse to the gustatory region of the cerebral cortex of the brain is transmitted.
		Taste cells membrane depolarization trigger ions influx. GPCRs or channel receptors regulates the release of neurotransmitters onto nerve fibres and/or from adjacent taste bud cells.
		Signal transduction cascades initiated taste receptors and stimulated by the chemical makeup of solutions.
		Liquid compounds, dissolved in saliva, interact with TRCs located on taste buds in the oral cavity, mostly on the tongue.



MEA = microelectrode array

Fig. 4. Diagram of tissue-based B-ET (A) with the pattern of 36 channel MEA (B) and intact taste epithelium to record extracellular potentials from taste buds. Reproduced with permission from (Liu et al., 2013c).

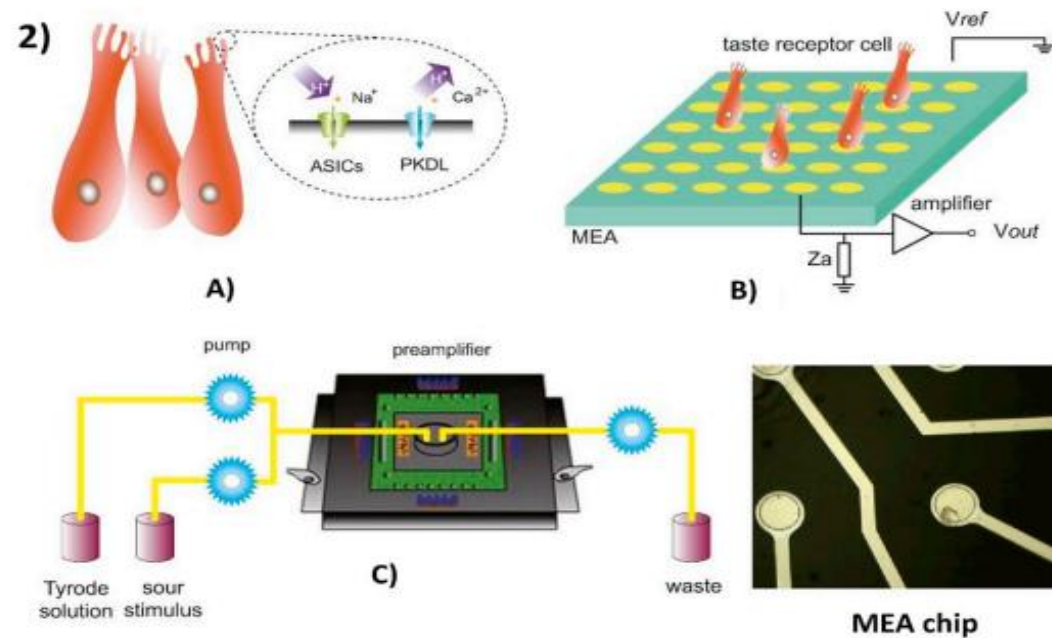
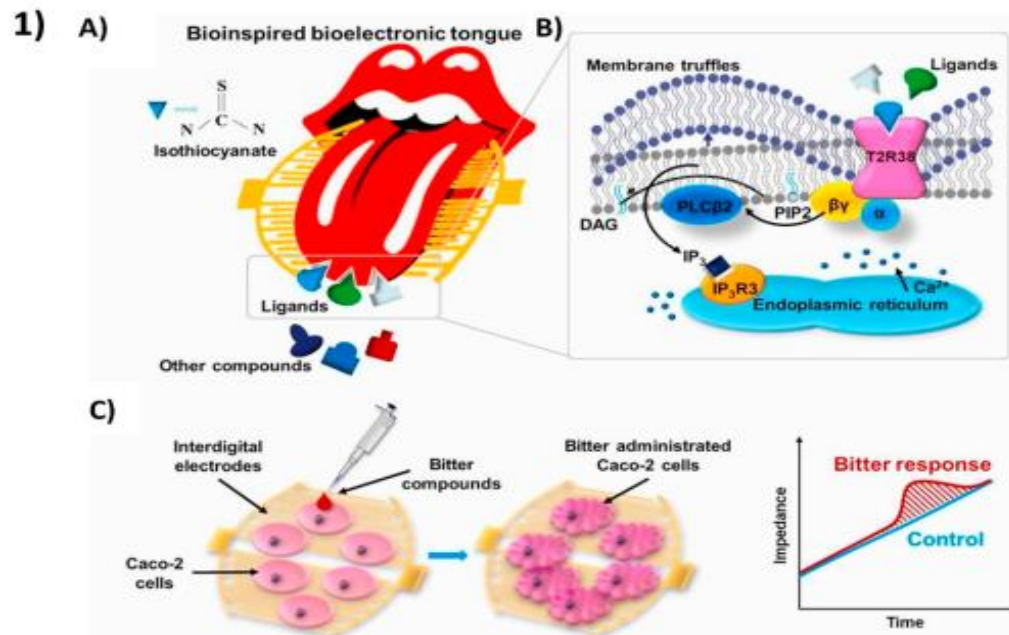


Fig. 5. Examples of cell-based biosensing instruments. (1) Schematic diagram showing cell-based bioinspired B-ET for iso-thiocyanates bitterness detection (A). Activation of the IP₃/DAG pathway induces increased intracellular Ca²⁺ and membrane truffles (B), application of bitter compounds induces morphological and attachment changes as well as increases cell-electrode impedance (C). Copyright with permission from (Qin et al., 2019). (2) A biomimetic whole-cell based B-ET with MEA transduction: A switch for On- and Off-response of acid sensations. Acid-sensing ion channels and Polycystic-kidney disease-like channels (A) for acid sensing biosensor design (B) by extracellular electrophysiological recordings of taste cells. Copyright with permission from (W. Zhang et al., 2017).